Table 1. Characteristics of lymphomas in *HBZ*-Tg and non-Tg littermates.

			Latency		IHC		
Genotype	**Strain**	**ID**	**(Months)**	**B220**	**CD3**	**Foxp3**	**Phenotype**
non-Tg			24	-	-	-	non-T, non-B
(2/27)			24	+	-	-	B
			26	+	-	-	B
			13	-	-	-	non-T, non-B
			27	-	+	+	T
			32	-	+	+	T
HBZ-Tg	#2	1	11	-	+	++	T
(14/37)	(3/14)	2	19	-	+	-	T
		3	24	-	+	+	T
	#9	1	23	+	+	+	T
	(4/5)	2	18	+	+	++	T
		3	26	+	+	+	T
		4	29	-	+	+	T
	#12	1	23	-	±	++	T
	(7/18)	2	19	-	+	+	T
		3	5	-	+	+++	T
		4	10	-	+	++	T
		5	27	+	+	-	T
		6	24	-	±	++	T
		7	18	-	+	+	T

Mice that died or became immobilized were subjected to autopsy. Tissue samples were surgically removed, fixed in 10% formalin in phosphate buffer, embedded in paraffin and stained with hematoxylin and eosin for histopathological examination. Tissue samples with lymphoma were subjected to immunohistochemical analysis (IHC) using monoclonal antibodies for CD3 (500A2), B220 (RA3-6B2), and Foxp3 (FJK-16s). The phenotype of lymphomas was determined based on CD3 and B220 expression. The degree of Foxp3 expression in lymphomas was evaluated by immunohistochemistry. (+, 1–9%; ++, 10–20%; +++, more than 20%) Frequency of T-cell lymphoma of each line is shown as follows; (number of T-cell lymphoma/number of total observed mice).

doi:10.1371/journal.ppat.1001274.t001

phenotype observed in *HBZ*-Tg mice (Figure 3, B and E). These findings prompted us to assess the possibility that HBZ might be involved in Foxp3-dependent transcriptional regulation. To address this, we first examined direct interaction among HBZ, NFAT and Foxp3. Immunoprecipitation experiments showed that HBZ physically interacted with both NFAT and Foxp3 (Figure 5A). Moreover, to study the interaction of endogenous HBZ and Foxp3, we performed immunoprecipitation using ATL-43T, a Foxp3-expressing ATL cell line. An anti-HBZ antibody co-precipitated endogenous Foxp3 in the ATL-43T cells, demonstrating that the interaction occurs not only in an enforced over-expressed state but also under physiological conditions (Figure 5B). It has been previously reported that human FoxP3 protein migrates as a doublet, which coincides with this result [38]. Analyses using HBZ deletion mutants showed that the central domain of HBZ interacted with Foxp3 (Figure 5C). Experiments with Foxp3 deletion mutants revealed that HBZ interacted with the forkhead (FH) domain of Foxp3 (Figure 5D). It has been reported that the region between the forkhead domain and the leucine zipper domain of Foxp3 interacted with AML-1 [36]. HBZ did not inhibit the binding between Foxp3 and AML-1 nor the suppressive effect of Foxp3 on AML-1-mediated transcription from the IL-2 gene promoter (Figure S11), indicating that HBZ does not influence Foxp3/AML1 mediated gene regulation.

To study whether HBZ independently interacts with Foxp3 and NFAT or, alternatively, if these molecules form a ternary complex, we studied the effect of the DNA intercalator ethidium bromide (EtBr) on their interactions. As shown in Figure 5E, the interactions of HBZ with Foxp3 or NFAT were not affected by EtBr while the interaction between NFAT and Foxp3 was diminished by EtBr as reported previously [35]. These findings suggest that the interactions of HBZ with NFAT and Foxp3 are independent of DNA while the interaction between NFAT and Foxp3 requires the presence of DNA.

HBZ inhibits Foxp3-mediated CTLA-4 and GITR expression in CD4$^+$ T cells *in vitro*

In *HBZ*-Tg mice, the expression of T_{reg}-associated molecules including CTLA-4, GITR and CD25 was suppressed when compared with their expression in T_{reg} cells from non-Tg mice (Figure 3B and E). This finding may account for the impaired function of T_{reg} cells since these molecules, in particular CTLA-4, play a critical role in T_{reg}-mediated suppression [39]. To further study the effect of HBZ on the expression of T_{reg}-associated molecules, we transduced HBZ along with Foxp3 into naive CD4$^+$ T cells *in vitro* using retrovirus vectors (Figure 4A). HBZ expression suppressed Foxp3-induced GITR and CTLA-4 expression whereas it did not inhibit CD25 expression (Figure 6A). Expression of HBZ alone increased CD25 expression (Figure 6A), which might obscure the suppressive effect of HBZ under these conditions. Suppression of GITR and CTLA-4 expression required both the activation and the central domains of HBZ (Figure 6, B and C), which correspond to the binding sites of HBZ to Foxp3 (Figure 5C) and NFAT (Figure S12). Since both Foxp3 and NFAT are critical

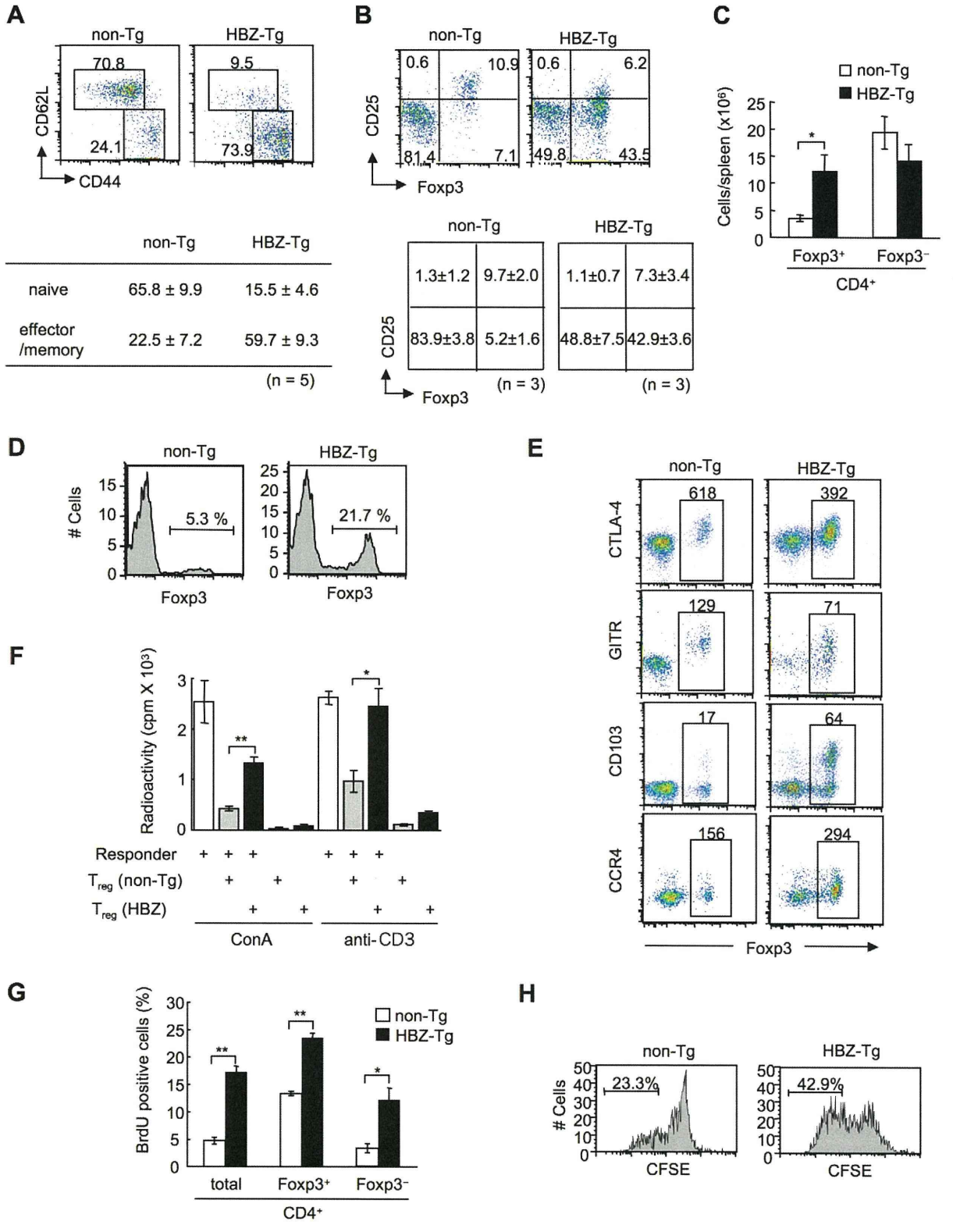

	non-Tg	HBZ-Tg
naive	65.8 ± 9.9	15.5 ± 4.6
effector /memory	22.5 ± 7.2	59.7 ± 9.3
	(n = 5)	

CD25 \ Foxp3	non-Tg		HBZ-Tg	
	1.3±1.2	9.7±2.0	1.1±0.7	7.3±3.4
	83.9±3.8	5.2±1.6	48.8±7.5	42.9±3.6
	(n = 3)		(n = 3)	

Figure 3. Transgenic expression of HBZ in CD4$^+$ T cells increases Foxp3$^+$ T$_{reg}$ cells with impaired suppressive function. (A and B) Mouse splenocytes were stained with the indicated antibodies, and analyzed by flow cytometry. Representative dot plots gated on the CD4$^+$ population are shown. For these experiments, *HBZ*-Tg mice without any symptoms were used. Tables show the mean ± SD (n = 5 for A, n = 3 for B). (C) The absolute number of Foxp3$^+$ or Foxp3$^-$ CD4$^+$ T cells in *HBZ*-Tg and non-Tg mice. The results shown are the mean ± SD (n = 3). (D) Flow cytometric analysis for the Foxp3 expression in CD4 single positive thymocytes. Representative dot plots gated on the CD4 single positive population are shown from three independent analyses. (E) Flow cytometric analyses of CD4$^+$ T cells for T$_{reg}$ related molecules. Numbers in dot plots indicate mean fluorescence intensity (MFI) of each molecule in the rectangular gates. (F) Suppressive activity of T$_{reg}$ cells from *HBZ*- or non-Tg mice on T-cell proliferation. Sorted Foxp3$^+$ T cells were cultured with CD4$^+$CD25$^-$ cells of non-Tg mice as responder cells for 72 h with ConA or soluble anti-CD3

antibody and x-irradiated antigen presenting cells (APCs), and [^{3}H] thymidine incorporation during the last 6 hours was measured. Results are means ± SD for triplicate cultures. (G) *In vivo* BrdU incorporation in total CD4$^+$, Foxp3$^+$CD4$^+$, or Foxp3$^-$CD4$^+$ T cells. The results shown are the mean ± SD (n = 3). (H) Sorted Foxp3$^+$ cells were labeled with CFSE and cultured with anti-CD3 antibody and x-irradiated APCs. After 96 hours, the cells were stained with anti-Foxp3, and CFSE dilution was analyzed for Foxp3$^+$ cells. *, $P<0.01$; **, $P<0.001$ by two-tailed Student *t*-test.
doi:10.1371/journal.ppat.1001274.g003

for T_{reg} function [35], it is likely that HBZ suppresses the expression of GITR and CTLA-4 by interacting with Foxp3 and NFAT and thereby interfering with their transcriptional regulation in T_{reg} cells. To examine suppressive effect of HBZ on expression of GITR, CTLA-4 and CD25, we isolated T_{reg} cells from wild type mice and expressed HBZ using retroviral vectors. As shown in Figure 6D, HBZ suppressed endogenous expression of CD25, GITR and CTLA-4 in T_{reg} cells, confirming that HBZ is responsible for suppressed expression of these molecules.

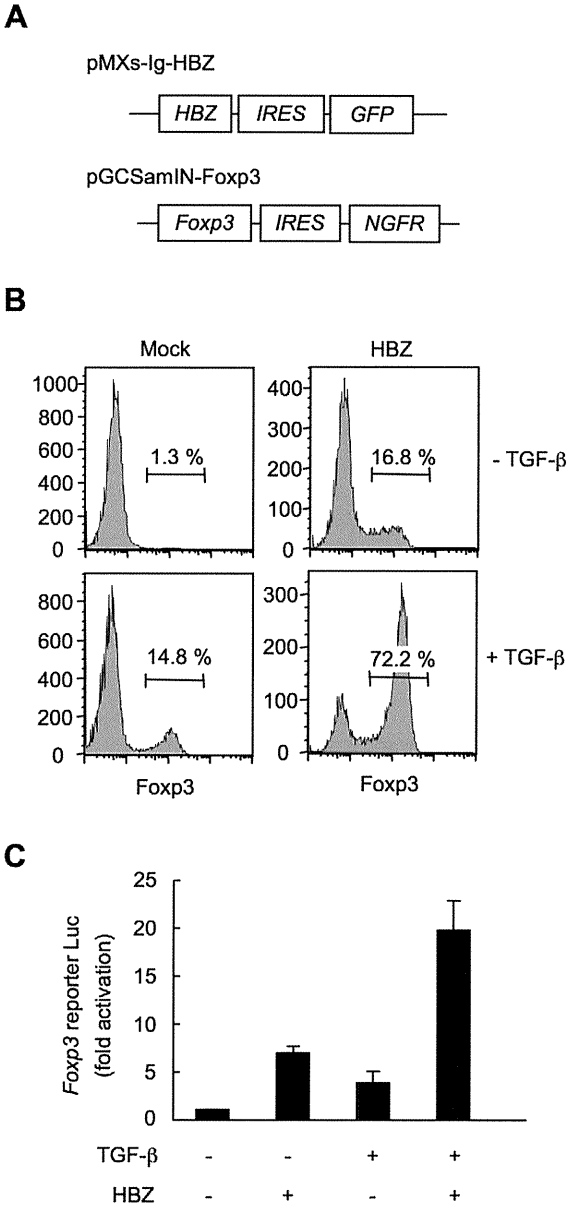

Figure 4. HBZ directly induces Foxp3 expression in CD4$^+$ T cells. (A) Schematic diagrams of retrovirus vectors used in this study. (B) Mouse CD4$^+$CD25$^-$ T cells transduced with retrovirus vector encoding HBZ or empty vector with or without TGF-β were stained with anti-Foxp3 antibody and analyzed by flow cytometry. (C) To study the effect of HBZ on promoter activity of the *Foxp3* gene, EL4 cells were transfected with Foxp3 reporter plasmid and/or HBZ expressing plasmid. Representative data shown are firefly luciferase activities normalized to those of renilla luciferase (mean ± SD).
doi:10.1371/journal.ppat.1001274.g004

Discussion

HTLV-1 targets CD4$^+$ T cells; cell central to immune regulation. In contrast to human immunodeficiency virus, which destroys CD4$^+$ T cells, HTLV-1 increases its copy number by inducing clonal proliferation of infected cells *in vivo* [40,41]. Since HTLV-1 spreads mainly by cell-to-cell transmission [5], increased number of infected cells facilitates transmission of HTLV-1 to new cells. Recent studies showed that glucose transporter 1, heparan sulfate proteoglycans and neuropilin-1 are important for the entry of HTLV-1[42,43,44], consistent with the finding that this virus can infect a variety of cell types [45,46]. However, HTLV-1 provirus is detected mainly in the regulatory and effector/memory CD4$^+$ T cells of HTLV-1 carriers (Figure S13) [25,26,27], which indicates that HTLV-1 favors these specific subpopulations of CD4$^+$ T cells. These findings suggest that HTLV-1 induces proliferation and/or facilitates survival of the regulatory and effector/memory CD4$^+$ T cells. The mechanism(s) by which HTLV-1 targets T_{reg} cells, however, remained unclear until now. In this study, we showed that HBZ could enhance transcription of the *Foxp3* gene, and also promote proliferation of Foxp3$^+$CD4$^+$ T cells in transgenic mice, indicating that HBZ enhances both the generation and proliferation of Foxp3$^+$ T cells. Impaired Foxp3 function is associated with proliferation of T_{reg} cells [37], so the HBZ-mediated T_{reg} dysfunction may also contribute to T_{reg} proliferation in addition to direct growth proliferation by the HBZ transcript [13]. Another possible explanation is that T_{reg} cells might be more susceptible to HTLV-1 infection, since T_{reg} cells proliferate vigorously *in vivo* presumably by recognizing self-antigen and commensal microbes [47]. With these strategies, HTLV-1 likely targets this specific T-cell population as its host, which might be beneficial for their survival.

As mechanisms of the HBZ-mediated effect on Foxp3 functions, we demonstrated that HBZ physically interacted with Foxp3 and impaired its function *in vitro*. HBZ lacking the Foxp3-binding region showed a slight inhibitory effect on Foxp3 function, indicating that direct interaction between HBZ and Foxp3 is, at least in part, responsible for suppression. The results of immunoprecipitation analyses using Foxp3 mutants showed that the forkhead domain of Foxp3 was responsible for the molecular interaction between HBZ and Foxp3. Since the forkhead domain is the DNA-binding domain of Foxp3 [17], HBZ might inhibit the transcriptional function of Foxp3 by interfering with the DNA binding activity. Foxp3 play a key role in the function and homeostasis of T_{reg} cells [22,23,24], indicating that HBZ-mediated dysfunction of Foxp3 contributes to impaired T_{reg} function in *HBZ*-Tg mice. This impaired T_{reg} function allows non-regulatory T cells to become hyper-reactive to commensal microbes and self-antigens, provoking enhanced proliferation of non-regulatory T cells and T cell-mediated autoimmune/inflammatory disease. These data collectively suggest that the viral protein HBZ hijacks the transcriptional

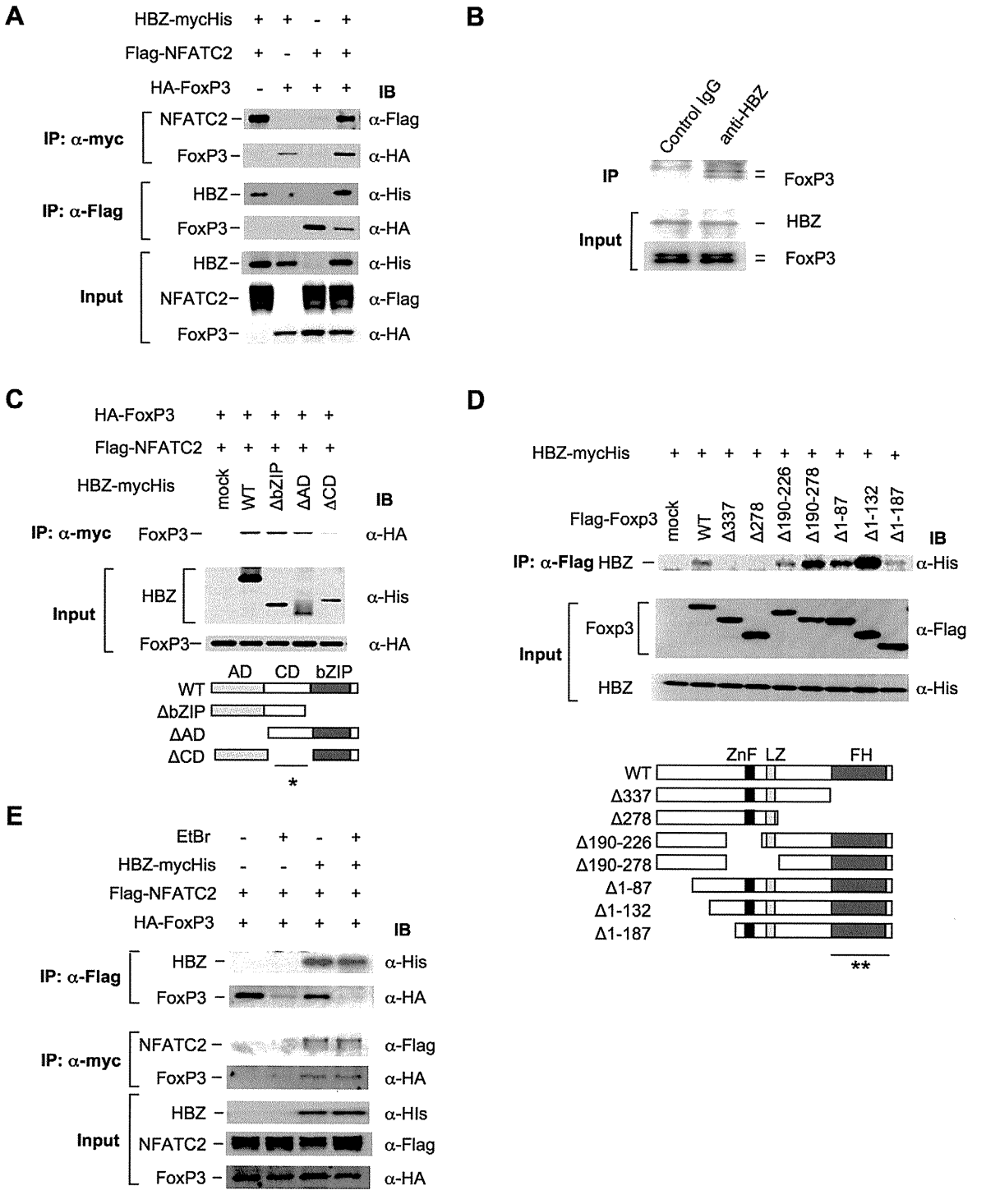

Figure 5. HBZ physically interacts with Foxp3 and NFAT. (A) The expression vectors of the indicated proteins were co-transfected into 293FT cells, and their interactions were analyzed by immunoprecipitation (IP). (B) Nuclear extract of ATL-43T cells was subjected to IP with anti-HBZ antibody or control IgG, and detected by anti-FoxP3 antibody. (C and D) The interactions of HBZ and Foxp3 were analyzed by IP using HBZ mutants (C) or Foxp3 mutants (D). A schematic diagram of Foxp3 mutants is shown. ZnF, zinc finger; LZ, leucine zipper; FH, forkhead domain. Asterisks (* or **) show responsible region for each molecular interaction. (E) The interactions among HBZ, Foxp3 and NFATc2 were analyzed with or without EtBr.
doi:10.1371/journal.ppat.1001274.g005

machinery of host T_{reg} cells leading to inflammatory disorders in the host. Conversely, Tax, another HTLV-1 protein, has been reported to suppress FoxP3 expression in human T cells *in vitro* [48]. Therefore, it is likely that both viral proteins target Foxp3 albeit with apparently different effects. Considering that HBZ is consistently expressed while Tax expression is sporadic, Tax might control excess expression of Foxp3 in HTLV-1 infected cells.

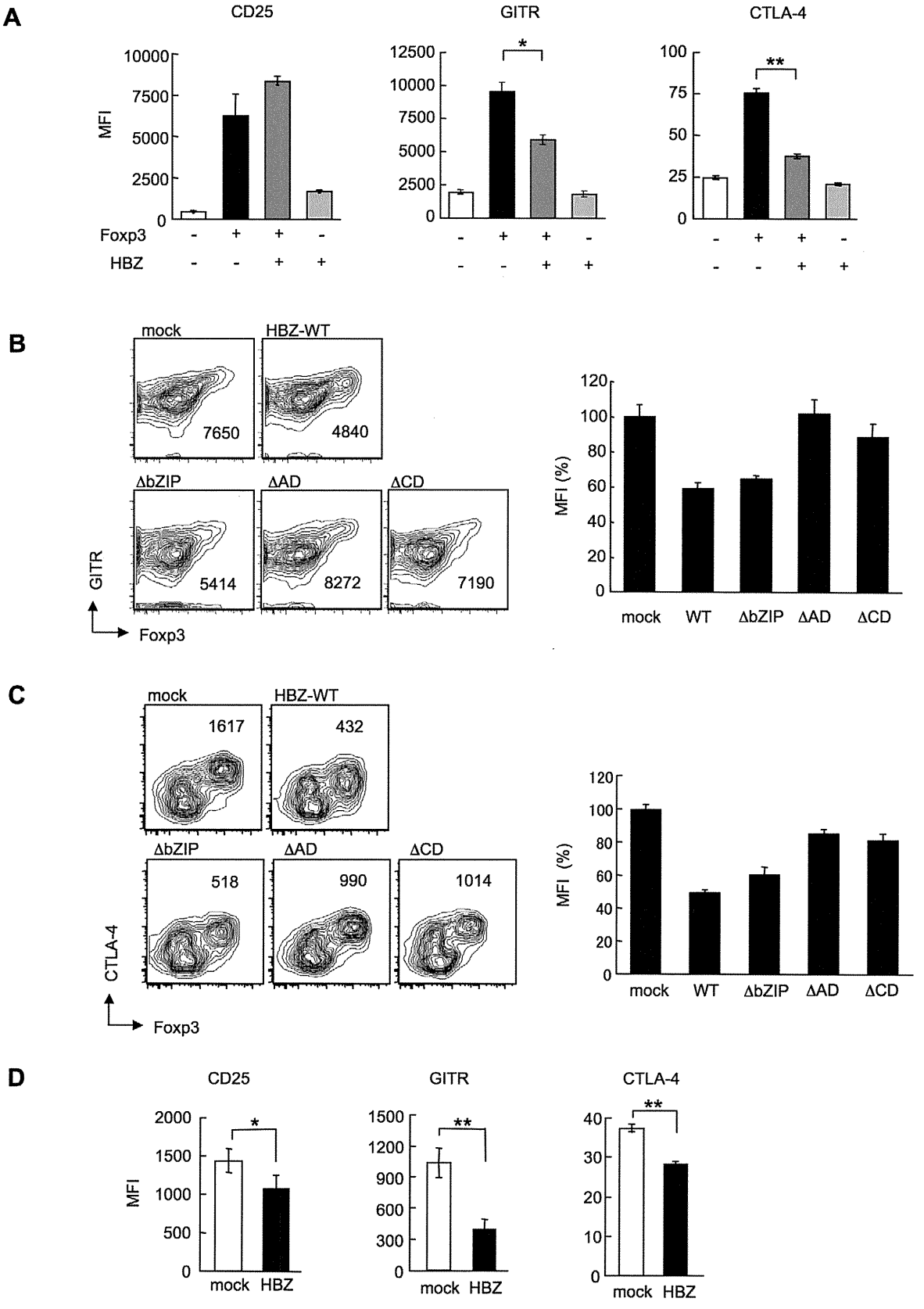

Figure 6. HBZ inhibites Foxp3-mediated CTLA-4 and GITR expression *in vitro*. (A) Mouse $CD4^{+}CD25^{-}$ T cells co-transduced with the retroviral vectors were stained with the indicated antibodies. Mean fluorescence intensity (MFI) of CD25, GITR, and CTLA-4 in GFP/NGFR double-positive cells are shown as mean ± SD. for triplicate culture. *, $P<0.01$; **, $P<0.001$ by two-tailed Student *t*-test. (B and C) $CD4^{+}CD25^{-}$ T cells transduced with the pMXs-Ig vector encoding wild-type or mutant HBZ, and pGCSamIN-Foxp3 vector were stained with anti-GITR (B) or anti-CTLA-4

(C) antibody in addition to anti-NGFR antibody, and then analyzed by flow cytometry. *Left*, numbers in density plots indicate MFI of GITR (B) or CTLA-4 (C) in GFP/NGFR double-positive cells. Representative data from three independent experiments are shown. *Right*, relative MFI of wild type or mutated HBZ compared to mock transduced cells was shown as mean ± SD (n = 3). (D) HBZ transduction in Foxp3$^+$ T_{reg} cells inhibited the endogenous expression of T_{reg} associated molecules. Mean fluorescence intensity (MFI) of CD25, GITR, and CTLA-4 in CD4$^+$Foxp3$^+$NGFR$^+$ cells are shown as mean ± SD. for triplicate culture. *, $P<0.05$; **, $P<0.01$ by two-tailed Student *t*-test.
doi:10.1371/journal.ppat.1001274.g006

In this study, we demonstrated that the characteristics of CD4$^+$ T cells in *HBZ*-Tg mice resemble those of human ATL cells or HTLV-1 infected cells in carriers. First, the frequency of Foxp3 positive cells in T-cell lymphomas was similar in *HBZ*-Tg mice and in ATL [20]. Second, the suppressive function of Foxp3$^+$ T cells was impaired in both ATL and *HBZ*-Tg mice [49]. Third, CD4$^+$ T cells in *HBZ*-Tg mice, HTLV-1-infected cells in carriers, and ATL cells possess similar effector/memory and regulatory phenotypes [25,27]. As shown in this study, transgenic mice expressing Tax under the same promoter as the *HBZ*-Tg mice did not show any changes in the number of Foxp3$^+$ T_{reg} cells or effector/memory T cells. These data suggest that HBZ, rather than Tax, is responsible for conferring the specific phenotype of HTLV-1 infected cells and ATL cells.

It has been reported that *tax* transgenic animals develop tumors [50,51,52]. In these reports, Tax induced tumors, the type of which depends on the promoter used. However, irrespective of the possible oncogenic activity of Tax, leukemic cells in ATL patients frequently lose Tax expression [7], whereas *HBZ* expression has been detected in all ATL cases studied so far [13]. We reported that the *HBZ* gene transcript itself has growth-promoting activity *in vitro* [13]. Taken together, our results suggest that HBZ is responsible for the specific phenotype, function and proliferation of HTLV-1-infected CD4$^+$ T cells and ATL cells, and that HBZ plays important roles for the oncogenic activity of HTLV-1 in addition to Tax. Further, the long latent period before the onset of T-cell lymphomas in *HBZ*-Tg mice suggests that additional genetic and/or epigenetic alterations in CD4$^+$ T cells are necessary for the development of T-cell lymphomas in *HBZ*-Tg mice as well as for ATL.

In conclusion, the HBZ-mediated dysregulation of T_{reg} function and proliferation that we report here provides novel insights into the interaction between the host and the virus and may be exploited to treat and prevent HTLV-1-induced diseases.

Materials and Methods

Ethics statement

This study was conducted according to the principles expressed in the Declaration of Helsinki. The study was approved by the Institutional Review Board of Kyoto University (E921). All patients provided written informed consent for the collection of samples and subsequent analysis. Animal experimentation was performed in strict accordance with the Japanese animal welfare bodies (Law No. 105 dated 19 October 1973 modified on 2 June 2006), and the Regulation on Animal Experimentation at Kyoto University. The protocol was approved by the Institutional Animal Research Committee of Kyoto University (Permit Number: D09-3). All efforts were made to minimize suffering.

Mice and cell cultures

C57BL/6J mice were purchased from CLEA Japan. The HBZ cDNA was cloned into the *Sal*I site of the H/M/T-CD4 vector, which was designed for restricted expression of a transgene in CD4$^+$ cells. The purified fragment containing the HBZ transgene was microinjected into C57BL/6J F1 fertilized eggs. Transgenic founders were screened for the integration of transgenes in their genomic DNA by PCR and mated with C57BL/6J mice to generate transgenic progeny [13,15]. All *HBZ*-Tg mice were heterozygotes for the transgene. The phenotype of *HBZ*-Tg mice was stable in the different generations. They express the spliced *HBZ* gene under the control of the *CD4*-specific promoter/enhancer/silencer. All mice were used at 10-16 weeks of age unless specifically described.

The human embryonic kidney cell line, 293FT, was cultured in DMEM containing 10% FCS and G418 (500 μg/ml). The 293FT cell line is derived from the 293F cell line and stably expresses the SV40 large T antigen. 293FT cell line was purchased from Invitrogen. The packaging cell line, Plat-E (kindly provided by T. Kitamura, Tokyo University) was cultured in DMEM supplemented with 10% FCS containing 10 μg/ml blasticidin and 1 μg/ml puromycin. ATL-43T(−) (kindly provided by M. Maeda, Kyoto University) and MT-1 cells were derived from ATL cells, and cultured in RPMI containing 10% FCS and antibiotics (penicillin and streptomycin). A mouse T-cell lymphoma line, EL4 cells, were cultured with RPMI1640 containing 10% FCS, antibiotics, and 50 μM 2-mercaptoethanol (2-ME; Invitrogen).

Plasmids

In order to construct the vectors expressing tagged spliced HBZ and its mutants, their coding sequences were amplified by PCR, and cloned into the expression vector, pcDNA 3.1(−)/myc-His (Invitrogen). A cDNA clone that contains NFATc2 coding sequence was kindly provided by Kazusa DNA Research Institute. To construct the FLAG-tagged NFATc2 expression vector, its coding region was cloned into pCMV-Tag2 (Stratagene). pCMV-HA (Clontech) was used to generate HA-tagged Foxp3 expression vectors. The vectors expressing Flag-tagged Foxp3 mutants were also used for immunoprecipitation.

Antibodies and reagents

The following antibodies were used for immunoprecipitation and Western blotting: mouse anti-Flag (clone M2; Sigma, Saint Louis, MO), mouse anti-c-myc (clone 9E10; Sigma), mouse anti-HA (clone HA-7; Sigma), rabbit anti-His polyclonal antibody (MBL), rabbit anti-FOXP3 (polyclonal antibody; Abcam), and rabbit anti-HBZ polyclonal antisera [15].

The following antibodies were purchased from BD PharMingen; purified monoclonal antibody (mAb) for mouse CD4 (RM4-5), CD8α (53-6.7), CD25 (PC61), CD44 (IM7), CD103 (M290), and IL-2 (JES6-5H4). Purified monoclonal antibodies for mouse GITR (DTA-1), CTLA-4 (UC10-4B9), CD62L (MEL-14), TCRβ (H57-597), TCRγδ (eBioGL3) and Foxp3 (FJK-16s) or human FoxP3 (236A/E7) were purchased from eBioscience. Anti-mouse CCR4 antibody (polyclonal antibody; Capralogics) and FITC-labeled anti-goat IgG antibody (Santa Cruz Biotechnology) were used for the detection of mouse CCR4. The following reagents were used for cell culture: anti-CD3ε antibody (145-2C11; R&D systems), Con A (Sigma), PMA (Sigma), and ionomycin (Sigma).

Synthesis of cDNA and semiquantitative RT-PCR

cDNAs were synthesized from 1 μg total RNA of purified mouse CD4$^+$ T cells by a reverse transcriptase SuperScript III and random primers according to the manufacturer's instructions

(Invitrogen). Spliced *HBZ* and *GAPDH* transcripts were quantified using RT-PCR. The primers used were as follows: s*HBZ* gene: 5′-TAAACTTACCTAGACGGCGG-3′ (sense), 5′-CTGCCGATCACGATGCGTTT -3′ (antisense); *GAPDH* gene: 5′-GTGGAGA TTGTTGCCATCAACG -3′ (sense) and 5′-AGAGGGGCCATCCACAGTCTT-3′ (antisense). PCR was performed in a PC-808 (Astec) under the following conditions: *HBZ*: 2 minutes at 95°C, followed by 26 cycles of 30 seconds at 95°C, 30 seconds at 59°C and 60 seconds at 72°C; *GAPDH:* 3 minutes at 95°C, followed by 35 cycles of 30 seconds at 95°C, 30 seconds at 61°C and 30 seconds at 72°C.

Quantitative RT-PCR

To quantify the expression level of *HBZ*, a TaqMan probe and primers for *HBZ* were designed. The sequences of primers and probe for *HBZ* were as follows; *HBZ* primers; 5′-GGACGCAGTTCAGGAGGCAC-3′ (sense) and 5′-CCTCCAAGGATAATAGCCCG-3′ (antisense); *HBZ* probe; 5′-CCTGTGCCATGCCCGGAGGACCTGC-3′. We used the TaqMan Gene expression Assay for *18S rRNA* (Applied Biosystems) as an internal control. Relative expression level of *HBZ* or *IL-2* was calculated with the delta delta Ct method.

Retroviral constructs and transduction

For retroviral gene transduction experiments, spliced HBZ cDNA was cloned into a retroviral vector, pMXs-Ig (a gift from T. Kitamura), to generate pMXs-Ig-HBZ. pGCSamIN (kindly provided from M. Onodera) and pGCSamIN-Foxp3 were used as previously described. Transfection of the packaging cell line, Plat-E, was performed as described. For retroviral transduction, $CD25^{-}CD4^{+}$ cells were enriched by a CD4 enrichment kit (BD Pharmingen) and were activated by 0.5 μg/ml anti-CD3 Ab and 50 U/ml rIL-2 in the presence of T-cell-depleted and x-irradiated (20Gy) C57BL/6J splenocytes as APCs in 12 well plates. After 16 hours, activated T cells were transduced with viral supernatant and 4 μg/ml polybrene, and centrifuged at 3,000 rpm for 60 min. Cells were cultured in medium supplemented with 50 U/ml rIL-2. Activation of naïve T cells by anti-CD3 antibody influenced expression of these molecules. Therefore, we analyzed their expression after influence by activation was lost [35]. Two days later, Foxp3-mediated CTLA-4 expression was detected by a flow cytometry, and five days later, expression of GITR or CD25 was analyzed. After two days, we stimulated the transduced cells with 50 ng/ml PMA and 1 μg/ml ionomycin in the presence of protein transport inhibitor (BD PharMingen) for 6 hours, and then analyzed intracellular IL-2 expression using intracellular cytokine staining kits (BD Pharmingen) according to the manufacturer's instructions.

To elucidate the effect of HBZ on endogenous expression of T_{reg} associated molecules, we transduced HBZ into $CD4^{+}Foxp3^{+}$ cells purified from mouse splenocytes. Three days after transduction, the expression levels of T_{reg} associated molecules were evaluated by a flow cytometry.

Preparation of splenocytes, flow cytometric analyses, cell sorting, and assays of regulatory T cells

Cell suspensions were prepared from murine spleens by forcing the organs through a nylon mesh, and splenic erythrocytes were eliminated with NH_4Cl. Proliferation of murine cells was measured by ^{3}H-thymidine uptake after 3 days of incubation in RPMI1640 medium supplemented with 10% FCS and 50 μM 2-ME. Flow cytometric analyses and cell sorting were carried out using a FACS CantoII or FACS Aria with Diva Software (BD Pharmingen) and the data was analyzed by FlowJo software (Treestar). For cell surface staining, 10^{6} cells were incubated with mAbs for 30 min at 4°C, and then analyzed. For intracellular staining, we used a mouse Foxp3 staining kit according to its protocol (eBioscience). To sort $Foxp3^{+}$ cells, suspended splenocytes were stained with mAb for CD4 and GITR, and the $CD4^{+}GITR^{high}$ fraction was sorted by FACS Aria. Purity of the sorted population was always >90% by re-analysis of Foxp3 staining. For the *ex vivo* proliferation assay of $Foxp3^{+}$ cells, carboxyfluorescein diacetate, succinimidyl ester (CFSE)(Molecular Probe) was used according to the manufacturer's instructions. $Foxp3^{+}$ T cells (2×10^{4}/well) were stimulated with anti-CD3 antibody (4 μg/ml) in round-bottomed 96-well plates in the presence of x-irradiated splenocytes as antigen presenting cells (APC; 5×10^{4}/well) for 96 hours. Then, cells were permeabilized, and stained with anti-Foxp3. CFSE dilution was analyzed by flow cytometry. To evaluate the suppressive activity of $Foxp3^{+}$ T cells sorted from *HBZ*-Tg or non-Tg mice, $Foxp3^{+}$ T cells (2×10^{4}/well) were cultured with $CD25^{-}CD4^{+}$ cells (2×10^{4}/well) and APCs (5×10^{4}/well) from wild-type mice for 72 h in the presence of soluble anti-CD3 (4 μg/ml) or Con A (1 μg/ml), and then [^{3}H] thymidine incorporation was measured.

BrdU staining

In vivo proliferation was measured by BrdU incorporation. BrdU (Nacalai Tesque) was dissolved in PBS (3 μg/ml), and then 200 μl was injected intraperitoneally into *HBZ*-Tg and non-transgenic mice twice a day for three days as reported previously [53]. BrdU incorporation in $CD4^{+}$, $CD8^{+}$, or $B220^{+}$ splenocytes was detected using FITC BrdU Flow Kits (BD Pharmingen) according to the manufacturer's instructions. Flow cytometric analyses were performed on a FACS CantoII with Diva Software (BD Pharmingen).

Foxp3 reporter assay

We constructed Foxp3 promoter and enhancer reporter plasmids as the previous report [34]. A murine T-cell line, EL4 cells (1×10^{7}), were transiently cotransfected by electroporation with the following plasmid DNAs: *Foxp3* reporter plasmid, *Renilla* luciferase control vector (pRL-TK), and HBZ expression vector (pME18SneoHBZ). Cells were cultured with or without TGF-β (2 ng/ml). Firefly and *Renilla* luciferase activities were measured using the Dual-Luciferase Reporter Assay System (Promega). Relative luciferase activities were calculated as the ratio of firefly and *Renilla* luciferase activities. The luciferase values are shown as relative values. Values represent means plus standard deviations (error bars) (n = 3).

Histological analyses

The study of clinical samples was approved by the local research ethics committee of the appropriate hospital. Tissue samples were fixed in 10% formalin in phosphate buffer and then embedded in paraffin. Haematoxylin and eosin (H&E) staining was performed according to standard procedures. Images were captured using a Provis AX80 microscope (Olympus) equipped with OLYMPUS DP70 digital camera, and detected using a DP manager system (Olympus).

For analysis of tumors, mice that became immobilized were sacrificed and subjected to autopsy. Tissue samples were surgically removed and fixed in 10% formalin in phosphate buffer and embedded in paraffin. Sections were stained with H&E for histopathologic examination. After we obtained informed consent, tissue samples from patients who were diagnosed as lymphoma-type ATL were analyzed by immunohistochemical methods to

determine FoxP3 expression. Monoclonal antibodies for CD3ε(500A2; BD Pharmingen), B220 (RA3-6B2; BD Pharmingen), and Foxp3 (FJK-16s; eBioscience) were used for immunohistochemistry. We judged $CD3^+B220^+$ cases to be T-cell lymphomas since some activated T cells and T cells of the *lpr/lpr* mutant mouse expressed B220 [54,55].

PCR/single stranded conformation polymorphism (SSCP) analysis

To investigate clonality of lymphoma cells observed in *HBZ*-Tg mice, lymphoma tissue samples of *HBZ*-Tg were analyzed for the clonality of T-cell receptor (TCR) γ locus using PCR-SSCP analysis of the TCR γ-gene. Genomic DNA was subjected to PCR amplification using primers for the Vγ2 gene and the Jγ1. The primers used were as follows: Vγ2: 5′-ACCAAGAGATGAGACTGCACAA-3′ (sense), Jγ1: 5′-GCGTCTGATCCTCAAAATAACTTCC-3′ (antisense); PCR was performed in a PC-808 (Astec) under the following conditions: 3 minutes at 95°C, followed by 35 cycles of 30 seconds at 95°C, 30 seconds at 55°C and 30 seconds at 72°C. We used EL-4 as a positive control and splenic DNA from young non-Tg or *HBZ*-Tg mice as negative control. PCR products were run on a 6% polyacrylamide gel and visualized by staining with DNA Silver Staining Kit (GE Healthcare).

Coimmunoprecipitation assay and immunoblotting

Expression vectors for the relevant genes were transiently cotransfected into 293FT cells using the TransIT-LT1 reagent (Mirus Bio). 24 hours later, transfected cells were stimulated with 50 ng/ml PMA and 1 μg/ml ionomycin for another 6 hours. Coimmunoprecipitation assays were performed using the Nuclear Complex Co-IP Kit (Active motif). Briefly, the nuclear extracts of transfected cells were prepared in the presence or absence of ethidium bromide (10 μg/ml). They were precleared with Protein G Sepharose 4 Fast Flow (GE Healthcare), and their supernatants were incubated with anti-myc tag (clone 9E10, Sigma) or anti-Flag tag (M2, Sigma) antibody overnight at 4°C. The immunocomplexes were precipitated with Protein G Sepharose 4 Fast Flow, fractionated in SDS-PAGE, and transferred to PVDF membranes. HBZ-myc-His was detected with horseradish peroxidase (HRP)-conjugated anti-His tag (MBL) antibody. HRP-conjugated anti-Flag tag (Sigma) and anti-HA tag (Sigma) antibodies were used to detect Flag-tagged and HA-tagged proteins, respectively. To detect endogenous interaction between HBZ and FoxP3, immunoprecipitation was performed using an ATL cell line, ATL-43T (-), as described above with anti-HBZ antisera and anti-FOXP3 antibody (Abcam). To examine the expression of HBZ in transgenic mice, $CD4^+$ splenocytes from wild type or *HBZ*-Tg mice were enriched by a mouse CD4 T lymphocyte enrichment set (Pharmingen). Whole cell extracts were prepared with the lysis buffer (50 mM Tris-HCL, PH 7.5, 150 mM NaCl, 1% NP-40), and analyzed by western blotting with anti-HBZ antisera.

Flow cytometric analysis for HTLV-1 carrier cells

A previous report demonstrated that Tax expression could not be detected in freshly isolated PBMC from HTLV-1 infected carriers but could be detected when they were cultivated *ex vivo* for 12 hours [56]. We cultured PBMCs from asymptomatic HTLV-1 carriers for 12 hours and stained with monoclonal antibodies against FoxP3 or Tax (MI-73), and then analyzed by flow cytometry.

Statistical analysis

For *in vitro* experiments, multiple data comparisons were performed using Student's unpaired *t*-test. Statistical differences in the incidence of T-cell lymphoma were analyzed using a logrank test.

Supporting Information

Figure S1 Characterization of the transgene. (A) Schematic structure of the transgene. (B) Copy numbers of the transgene in each line were determined by Southern blot analysis. Serially diluted plasmids, used to calculate the copy number, are shown on the left side.
Found at: doi:10.1371/journal.ppat.1001274.s001 (0.35 MB TIF)

Figure S2 Histological analysis of the skin and lung of *HBZ*-Tg mice. HE staining showed massive infiltration of lymphocytes in *HBZ*-Tg line 9 and 12, but not in line 2. Immunohistochemical staining revealed that only some of infiltrating lymphocytes were FoxP3 positive. Arrows indicate FoxP3 positive cells.
Found at: doi:10.1371/journal.ppat.1001274.s002 (4.46 MB TIF)

Figure S3 Flow cytometric analysis of TCRβ and TCR γδ expression in the spleen with lymphoma observed in *HBZ*-Tg mice. Numbers are identical to those of Table 1.
Found at: doi:10.1371/journal.ppat.1001274.s003 (0.32 MB TIF)

Figure S4 PCR/single stranded conformation polymorphism (SSCP) analysis. *HBZ*-Tg lymphoma tissue samples were analyzed for TCR clonality using PCR-SSCP analysis of the TCR γ-gene. EL-4 are shown as a positive control and splenic DNA from young (less than 6 weeks old) non-Tg or *HBZ*-Tg mice as a negative control. Lanes 1- 5 (#2-3, #9-1, #12-6, #9-3, #12-7) show lymphoma from *HBZ*-Tg mice respectively (Table 1).
Found at: doi:10.1371/journal.ppat.1001274.s004 (1.09 MB TIF)

Figure S5 Analysis of FoxP3 expression in fresh ATL cells. Immunohistochemical staining for FoxP3 in the lymph nodes of human ATL patients. We used a monoclonal antibody for human FoxP3 (236A/E7; eBioscience).
Found at: doi:10.1371/journal.ppat.1001274.s005 (1.89 MB TIF)

Figure S6 Flow cytometric analysis of thymocyte subsets. Non-Tg or *HBZ*-Tg thymocytes were stained with anti-CD4 and anti-CD8 antibody, and then analyzed by flow cytometry.
Found at: doi:10.1371/journal.ppat.1001274.s006 (0.48 MB TIF)

Figure S7 Foxp3 expression in spleen, cervical lymph node, or peripheral blood mononuclear cells was determined by flow cyotmetry. Representative histograms gated on the $CD4^+$ population are shown.
Found at: doi:10.1371/journal.ppat.1001274.s007 (0.36 MB TIF)

Figure S8 *HBZ*-Tg line 2 also showed an increase in effector/memory and regulatory CD4 T cells. Mouse splenocytes were stained with antibodies for CD4 and CD8 plus CD44 and CD62L (A) or CD25 and Foxp3 (B), and then analyzed by flow cytometry. Representative dot plots gated on the $CD4^+$ population are shown.
Found at: doi:10.1371/journal.ppat.1001274.s008 (0.57 MB TIF)

Figure S9 IL-2 production of $CD4^+$ T cells in *HBZ*-Tg mice. (A) Mouse splenocytes were stimulated with Leukocyte Activation Cocktail, which contains PMA/Ionomycin and protein transport inhibitor (BD Pharmingen), for 4 hours and then analyzed for intracellular IL-2 gated on the $CD4^+$ cells by flow cytometry. Representative results of more than three independent experiments are shown. (B) The percentage of $IL\text{-}2^+$ cells among $Foxp3^+$ cells is shown. The results shown are the mean ± SD of triplicate experiments.
Found at: doi:10.1371/journal.ppat.1001274.s009 (0.26 MB TIF)

Figure S10 Flow cytometric analyses of *tax*-Tg mice. Non-Tg or *tax*-Tg splenocytes were stained with the indicated antibodies, and analyzed by flow cytometry. Representative dot plots gated on the $CD4^+$ population are shown.
Found at: doi:10.1371/journal.ppat.1001274.s010 (0.54 MB TIF)

Figure S11 The effect of HBZ on Foxp3/AML-1 complex. (A) 293FT-cells were co-transfected with vectors expressing the indicated proteins, lysed, and subjected to immunoprecipitation. (B) Jurkat cells were co-transfected with expression vectors for the indicated proteins and IL-2 promoter-luc constructs. The results shown are relative values of firely luciferase normalized to Renilla luciferase and expressed as means ± SD. The experiments were repeated three times with similar results.
Found at: doi:10.1371/journal.ppat.1001274.s011 (0.37 MB TIF)

Figure S12 Characterization of the interaction between HBZ and NFAT. To investigate the region responsible for each interaction, we performed immunoprecipitation experiments with NFATC2 and deletion mutants of HBZ. Asterisk shows the region responsible for the molecular interaction.
Found at: doi:10.1371/journal.ppat.1001274.s012 (0.25 MB TIF)

Figure S13 The percentages of HTLV-1^+ T cells in $CD4^+FoxP3^-$ and $CD4^+FoxP3^+$ subpopulations of asymptomatic HTLV-1 carriers. It has been reported that ex vivo culture induces the reactivation of viral antigen in HTLV-1 infected cells. We cultured freshly isolated PBMC from two asymptomatic HTLV-1 carriers for 18 hours, and then stained intracellular Tax as a viral antigen to detect the presence of HTLV-1 by using a monoclonal antibody of Tax (MI-73).
Found at: doi:10.1371/journal.ppat.1001274.s013 (0.31 MB TIF)

Table S1 (A) Summary of BrdU incorporation *in vivo*. Data shown are percentage of BrdU positive cells of three different non-Tg or *HBZ*-Tg mice. (B) MFI of Treg associated molecules (CTLA-4, GITR, CD103, or CCR4) in non-Tg or *HBZ*-Tg (line 12) mice are shown as mean ± SD (n = 3). of three mice. *, $P<0.05$; **, $P<0.01$ by two-tailed Student t-test.
Found at: doi:10.1371/journal.ppat.1001274.s014 (0.25 MB TIF)

Acknowledgments

We thank A. Koito for H/M/T-CD4 vector; T. Kitamura for the pMXs-Ig vector and Plat-E cell; M. Onodera for the pGCSamIN vector; and J. Tanabe and A. Kamamoto for technical assistance, and Aaron Coutts and Kate Hayes-Ozello for editorial comments.

Author Contributions

Conceived and designed the experiments: YS JY MM. Performed the experiments: YS JY TZ MY PM KT KS KO. Analyzed the data: YS KO NO SS MM. Contributed reagents/materials/analysis tools: PLG TY MO. Wrote the paper: YS JY PLG NO SS MM.

References

1. Takatsuki K (2005) Discovery of adult T-cell leukemia. Retrovirology 2: 16.
2. Gallo RC (2005) The discovery of the first human retrovirus: HTLV-1 and HTLV-2. Retrovirology 2: 17.
3. Gessain A, Barin F, Vernant JC, Gout O, Maurs L, et al. (1985) Antibodies to human T-lymphotropic virus type-I in patients with tropical spastic paraparesis. Lancet 2: 407–410.
4. Osame M, Usuku K, Izumo S, Ijichi N, Amitani H, et al. (1986) HTLV-I associated myelopathy, a new clinical entity. Lancet 1: 1031–1032.
5. Igakura T, Stinchcombe JC, Goon PK, Taylor GP, Weber JN, et al. (2003) Spread of HTLV-I between lymphocytes by virus-induced polarization of the cytoskeleton. Science 299: 1713–1716.
6. Pais-Correia AM, Sachse M, Guadagnini S, Robbiati V, Lasserre R, et al. (2010) Biofilm-like extracellular viral assemblies mediate HTLV-1 cell-to-cell transmission at virological synapses. Nat Med 16: 83–89.
7. Matsuoka M, Jeang KT (2007) Human T-cell leukaemia virus type 1 (HTLV-1) infectivity and cellular transformation. Nat Rev Cancer 7: 270–280.
8. Journo C, Douceron E, Mahieux R (2009) HTLV gene regulation: because size matters, transcription is not enough. Future Microbiol 4: 425–440.
9. Grassmann R, Aboud M, Jeang KT (2005) Molecular mechanisms of cellular transformation by HTLV-1 Tax. Oncogene 24: 5976–5985.
10. Lairmore MD, Silverman L, Ratner L (2005) Animal models for human T-lymphotropic virus type 1 (HTLV-1) infection and transformation. Oncogene 24: 6005–6015.
11. Larocca D, Chao LA, Seto MH, Brunck TK (1989) Human T-cell leukemia virus minus strand transcription in infected T-cells. Biochem Biophys Res Commun 163: 1006–1013.
12. Gaudray G, Gachon F, Basbous J, Biard-Piechaczyk M, Devaux C, et al. (2002) The complementary strand of the human T-cell leukemia virus type 1 RNA genome encodes a bZIP transcription factor that down-regulates viral transcription. J Virol 76: 12813–12822.
13. Satou Y, Yasunaga J, Yoshida M, Matsuoka M (2006) HTLV-I basic leucine zipper factor gene mRNA supports proliferation of adult T cell leukemia cells. Proc Natl Acad Sci U S A 103: 720–725.
14. Fan J, Ma G, Nosaka K, Tanabe J, Satou Y, et al. (2010) APOBEC3G generates nonsense mutations in human T-cell leukemia virus type 1 proviral genomes in vivo. J Virol 84: 7278–7287.
15. Arnold J, Zimmerman B, Li M, Lairmore MD, Green PL (2008) Human T-cell leukemia virus type-1 antisense-encoded gene, Hbz, promotes T-lymphocyte proliferation. Blood 112: 3788–3797.
16. Saito M, Matsuzaki T, Satou Y, Yasunaga J, Saito K, et al. (2009) In vivo expression of the HBZ gene of HTLV-1 correlates with proviral load, inflammatory markers and disease severity in HTLV-1 associated myelopathy/tropical spastic paraparesis (HAM/TSP). Retrovirology 6: 19.
17. Sakaguchi S, Yamaguchi T, Nomura T, Ono M (2008) Regulatory T cells and immune tolerance. Cell 133: 775–787.
18. Hattori T, Uchiyama T, Toibana T, Takatsuki K, Uchino H (1981) Surface phenotype of Japanese adult T-cell leukemia cells characterized by monoclonal antibodies. Blood 58: 645–647.
19. Uchiyama T, Hori T, Tsudo M, Wano Y, Umadome H, et al. (1985) Interleukin-2 receptor (Tac antigen) expressed on adult T cell leukemia cells. J Clin Invest 76: 446–453.
20. Karube K, Ohshima K, Tsuchiya T, Yamaguchi T, Kawano R, et al. (2004) Expression of FoxP3, a key molecule in CD4CD25 regulatory T cells, in adult T-cell leukaemia/lymphoma cells. Br J Haematol 126: 81–84.
21. Toulza F, Nosaka K, Takiguchi M, Pagliuca T, Mitsuya H, et al. (2009) FoxP3+ regulatory T cells are distinct from leukemia cells in HTLV-1-associated adult T-cell leukemia. Int J Cancer 125: 2375–2382.
22. Fontenot JD, Gavin MA, Rudensky AY (2003) Foxp3 programs the development and function of CD4+CD25+ regulatory T cells. Nat Immunol 4: 330–336.
23. Hori S, Nomura T, Sakaguchi S (2003) Control of regulatory T cell development by the transcription factor Foxp3. Science 299: 1057–1061.
24. Khattri R, Cox T, Yasayko SA, Ramsdell F (2003) An essential role for Scurfin in CD4+CD25+ T regulatory cells. Nat Immunol 4: 337–342.
25. Yasunaga J, Sakai T, Nosaka K, Etoh K, Tamiya S, et al. (2001) Impaired production of naive T lymphocytes in human T-cell leukemia virus type I-infected individuals: its implications in the immunodeficient state. Blood 97: 3177–3183.
26. Toulza F, Heaps A, Tanaka Y, Taylor GP, Bangham CR (2008) High frequency of CD4+FoxP3+ cells in HTLV-1 infection: inverse correlation with HTLV-1-specific CTL response. Blood 111: 5047–5053.
27. Richardson JH, Edwards AJ, Cruickshank JK, Rudge P, Dalgleish AG (1990) In vivo cellular tropism of human T-cell leukemia virus type 1. J Virol 64: 5682–5687.
28. Sugimoto M, Nakashima H, Watanabe S, Uyama E, Tanaka F, et al. (1987) T-lymphocyte alveolitis in HTLV-I-associated myelopathy. Lancet 2: 1220.
29. Bittencourt AL, de Oliveira Mde F (2010) Cutaneous manifestations associated with HTLV-1 infection. Int J Dermatol 49: 1099–1110.
30. Fontenot JD, Rasmussen JP, Gavin MA, Rudensky AY (2005) A function for interleukin 2 in Foxp3-expressing regulatory T cells. Nat Immunol 6: 1142–1151.
31. Sakaguchi S (2005) Naturally arising Foxp3-expressing CD25+CD4+ regulatory T cells in immunological tolerance to self and non-self. Nat Immunol 6: 345–352.
32. Lehmann J, Huehn J, de la Rosa M, Maszyna F, Kretschmer U, et al. (2002) Expression of the integrin alpha Ebeta 7 identifies unique subsets of CD25+ as well as CD25- regulatory T cells. Proc Natl Acad Sci U S A 99: 13031–13036.
33. Sather BD, Treuting P, Perdue N, Miazgowicz M, Fontenot JD, et al. (2007) Altering the distribution of Foxp3(+) regulatory T cells results in tissue-specific inflammatory disease. J Exp Med 204: 1335–1347.

34. Tone Y, Furuuchi K, Kojima Y, Tykocinski ML, Greene MI, et al. (2008) Smad3 and NFAT cooperate to induce Foxp3 expression through its enhancer. Nat Immunol 9: 194–202.
35. Wu Y, Borde M, Heissmeyer V, Feuerer M, Lapan AD, et al. (2006) FOXP3 controls regulatory T cell function through cooperation with NFAT. Cell 126: 375–387.
36. Ono M, Yaguchi H, Ohkura N, Kitabayashi I, Nagamura Y, et al. (2007) Foxp3 controls regulatory T-cell function by interacting with AML1/Runx1. Nature 446: 685–689.
37. Chae WJ, Henegariu O, Lee SK, Bothwell AL (2006) The mutant leucine-zipper domain impairs both dimerization and suppressive function of Foxp3 in T cells. Proc Natl Acad Sci U S A 103: 9631–9636.
38. Walker MR, Kasprowicz DJ, Gersuk VH, Benard A, Van Landeghen M, et al. (2003) Induction of FoxP3 and acquisition of T regulatory activity by stimulated human CD4+CD25- T cells. J Clin Invest 112: 1437–1443.
39. Wing K, Onishi Y, Prieto-Martin P, Yamaguchi T, Miyara M, et al. (2008) CTLA-4 control over Foxp3+ regulatory T cell function. Science 322: 271–275.
40. Wattel E, Vartanian JP, Pannetier C, Wain-Hobson S (1995) Clonal expansion of human T-cell leukemia virus type I-infected cells in asymptomatic and symptomatic carriers without malignancy. J Virol 69: 2863–2868.
41. Etoh K, Tamiya S, Yamaguchi K, Okayama A, Tsubouchi H, et al. (1997) Persistent clonal proliferation of human T-lymphotropic virus type I-infected cells in vivo. Cancer Res 57: 4862–4867.
42. Manel N, Kim FJ, Kinet S, Taylor N, Sitbon M, et al. (2003) The ubiquitous glucose transporter GLUT-1 is a receptor for HTLV. Cell 115: 449–459.
43. Jones KS, Petrow-Sadowski C, Bertolette DC, Huang Y, Ruscetti FW (2005) Heparan sulfate proteoglycans mediate attachment and entry of human T-cell leukemia virus type 1 virions into CD4+ T cells. J Virol 79: 12692–12702.
44. Lambert S, Bouttier M, Vassy R, Seigneuret M, Petrow-Sadowski C, et al. (2009) HTLV-1 uses HSPG and neuropilin-1 for entry by molecular mimicry of VEGF165. Blood 113: 5176–5185.
45. Koyanagi Y, Itoyama Y, Nakamura N, Takamatsu K, Kira J, et al. (1993) In vivo infection of human T-cell leukemia virus type I in non-T cells. Virology 196: 25–33.
46. Jones KS, Petrow-Sadowski C, Huang YK, Bertolette DC, Ruscetti FW (2008) Cell-free HTLV-1 infects dendritic cells leading to transmission and transformation of CD4(+) T cells. Nat Med 14: 429–436.
47. Vukmanovic-Stejic M, Zhang Y, Cook JE, Fletcher JM, McQuaid A, et al. (2006) Human CD4+ CD25hi Foxp3+ regulatory T cells are derived by rapid turnover of memory populations in vivo. J Clin Invest 116: 2423–2433.
48. Yamano Y, Takenouchi N, Li HC, Tomaru U, Yao K, et al. (2005) Virus-induced dysfunction of CD4+CD25+ T cells in patients with HTLV-I-associated neuroimmunological disease. J Clin Invest 115: 1361–1368.
49. Shimauchi T, Kabashima K, Tokura Y (2008) Adult T-cell leukemia/lymphoma cells from blood and skin tumors express cytotoxic T lymphocyte-associated antigen-4 and Foxp3 but lack suppressor activity toward autologous CD8+ T cells. Cancer Sci 99: 98–106.
50. Nerenberg M, Hinrichs SH, Reynolds RK, Khoury G, Jay G (1987) The tat gene of human T-lymphotropic virus type 1 induces mesenchymal tumors in transgenic mice. Science 237: 1324–1329.
51. Grossman WJ, Kimata JT, Wong FH, Zutter M, Ley TJ, et al. (1995) Development of leukemia in mice transgenic for the tax gene of human T-cell leukemia virus type I. Proc Natl Acad Sci U S A 92: 1057–1061.
52. Hasegawa H, Sawa H, Lewis MJ, Orba Y, Sheehy N, et al. (2006) Thymus-derived leukemia-lymphoma in mice transgenic for the Tax gene of human T-lymphotropic virus type I. Nat Med 12: 466–472.
53. von Boehmer H, Hafen K (1993) The life span of naive alpha/beta T cells in secondary lymphoid organs. J Exp Med 177: 891–896.
54. Asano T, Tomooka S, Serushago BA, Himeno K, Nomoto K (1988) A new T cell subset expressing B220 and CD4 in lpr mice: defects in the response to mitogens and in the production of IL-2. Clin Exp Immunol 74: 36–40.
55. Ishimoto Y, Tomiyama-Miyaji C, Watanabe H, Yokoyama H, Ebe K, et al. (2004) Age-dependent variation in the proportion and number of intestinal lymphocyte subsets, especially natural killer T cells, double-positive CD4+ CD8+ cells and B220+ T cells, in mice. Immunology 113: 371–377.
56. Hanon E, Hall S, Taylor GP, Saito M, Davis R, et al. (2000) Abundant tax protein expression in CD4+ T cells infected with human T-cell lymphotropic virus type I (HTLV-I) is prevented by cytotoxic T lymphocytes. Blood 95: 1386–1392.

研究成果の刊行に関する一覧表

研究分担者　京都大学医学研究科　附属ゲノム医学センター　松田　文彦

雑誌

発表者氏名	論文タイトル名	発表誌名	巻号	ページ	出版年
Nakata, I., Yamashiro, K., Yamada, R., Gotoh, N., Nakanishi, H., Hayashi, H., Tsujikawa, A., Otani, A., Saito, M., Iida, T., Oishi, A., Matsuo, K., Tajima, K., Matsuda, F. and Yoshimura, N.	Association between the *SERPING1* Gene and Age-Related Macular Degeneration and Polypoidal Choroidal Vasculopathy in Japanese	PLoS One	6	e19108	2011
Terao, C., Ohmura, K., Katayama, M., Takahashi, M., Kokubo, M., Diop, G., Toda, T., Yamamoto, N., Human Disease Genomics Working Group, RA Clinical and Genetic Study Consortium, Shinkura, R., Shimizu, M., Gut, I., Heath, S., Melchers, I., Manabe, T., Lathrop, M., Mimori, T., Yamada, R. and Matsuda, F.	Myelin basic protein as a novel genetic risk factor in rheumatoid arthritis - A genome-wide study combined with immunological analyses	PLoS One	6	e20457	2011
Toyoda, H., Kumada, T., Tada, T., Hayashi, K., Honda, T., Katano, Y., Goto, H., Kawaguchi, T., Murakami, Y. and Matsuda F.	Predictive value of early viral dynamics during peginterferon and ribavirin combination therapy based on genetic polymorphisms near the IL28B gene in patients infected with HCV genotype 1b.	J. Med. Virol.	84	61-70	2012
Kato, L., Beguma, N. A., Burroughs, M., Doi, T., Kawai, J., Daub, C. O., Kawaguchi, T., Matsuda, F., Hayashizaki, Y. and Honjo, T.	Nonimmunoglobulin target loci of activation-induced cytidine deaminase (AID) share unique features with immunoglobulin genes	Proc. Natl., Acad. Sci. U. S. A.	109	2479-2484	2012

OPEN ACCESS Freely available online

PLoS one

Association between the SERPING1 Gene and Age-Related Macular Degeneration and Polypoidal Choroidal Vasculopathy in Japanese

Isao Nakata[1,2], Kenji Yamashiro[1]*, Ryo Yamada[2], Norimoto Gotoh[1,2], Hideo Nakanishi[1,2], Hisako Hayashi[1,2], Akitaka Tsujikawa[1], Atsushi Otani[1], Masaaki Saito[3], Tomohiro Iida[3], Akio Oishi[4], Keitaro Matsuo[5], Kazuo Tajima[5], Fumihiko Matsuda[2], Nagahisa Yoshimura[1]

1 Department of Ophthalmology and Visual Sciences, Kyoto University Graduate School of Medicine, Kyoto, Japan, **2** Center for Genomic Medicine/Inserm U.852, Kyoto University Graduate School of Medicine, Kyoto, Japan, **3** Department of Ophthalmology, Fukushima Medical University, Fukushima, Japan, **4** Department of Ophthalmology, Kobe City Medical Center General Hospital, Kobe, Japan, **5** Division of Epidemiology and Prevention, Aichi Cancer Center Research Institute, Nagoya, Japan

Abstract

Purpose: Recently, a complement component 1 inhibitor (*SERPING1*) gene polymorphism was identified as a novel risk factor for age-related macular degeneration (AMD) in Caucasians. We aimed to investigate whether variations in *SERPING1* are associated with typical AMD or with polypoidal choroidal vasculopathy (PCV) in a Japanese population.

Methods: We performed a case-control study in a group of Japanese patients with typical AMD (n = 401) or PCV (n = 510) and in 2 independent control groups—336 cataract patients without age-related maculopathy and 1,194 healthy Japanese individuals. Differences in the observed genotypic distribution between the case and control groups were tested using chi-square test for trend. Age and gender were adjusted using logistic regression analysis.

Results: We targeted rs2511989 as the haplotype-tagging single nucleotide polymorphism (SNP) for the *SERPING1* gene, which was reported to be associated with the risk of AMD in Caucasians. Although we compared the genotypic distributions of rs2511989 in typical AMD and PCV patients against 2 independent control groups (cataract patients and healthy Japanese individuals), *SERPING1* rs2511989 was not significantly associated with typical AMD (P = 0.932 and 0.513, respectively) or PCV (P = 0.505 and 0.141, respectively). After correction for age and gender differences based on a logistic regression model, the difference in genotypic distributions remained insignificant (P>0.05). Our sample size had a statistical power of more than 90% to detect an association of a risk allele with an odds ratio reported in the original studies for rs2511989 for developing AMD.

Conclusions: In the present study, we could not replicate the reported association between *SERPING1* and either neovascular AMD or PCV in a Japanese population; thus, the results suggest that *SERPING1* does not play a significant role in the risk of developing AMD or PCV in Japanese.

Citation: Nakata I, Yamashiro K, Yamada R, Gotoh N, Nakanishi H, et al. (2011) Association between the SERPING1 Gene and Age-Related Macular Degeneration and Polypoidal Choroidal Vasculopathy in Japanese. PLoS ONE 6(4): e19108. doi:10.1371/journal.pone.0019108

Editor: Eric J. Kremer, French National Centre for Scientific Research, France

Received November 10, 2010; **Accepted** March 17, 2011; **Published** April 19, 2011

Funding: The study was supported in part by grants-in-aid for scientific research (Nos. 19390442, 22791706, and 27091294) from the Japan Society for the Promotion of Science, Tokyo, Japan, and by the Japanese National Society for the Prevention of Blindness. No additional external funding received for this study. The funders had no role in study design, data collection and analysis, decision to publish, or preparation of the manuscript.

Competing Interests: The authors have declared that no competing interests exist.

* E-mail: yamashro@kuhp.kyoto-u.ac.jp

Introduction

Age-related macular degeneration (AMD) is the leading cause of visual loss in the developed world [1]. Several genes have been reported to be associated with this disease, including complement factor H [2–4] and the age-related maculopathy susceptibility 2/HtrA serine peptidase 1 (ARMS2/HTRA1) region [5,6], and subsequent studies have replicated the association between susceptibility genes and the development of AMD using a different ethnic cohort [7–10].

Inner choroidal vascular networks that terminate in polypoidal lesions are defined as polypoidal choroidal vasculopathy (PCV), and are typically visualized by indocyanine green angiography [11]. Whether PCV represents a subtype of neovascular AMD remains controversial; moreover, whether this condition represents inner choroidal vascular abnormalities or is a variety of choroidal neovascularization remains unknown [12]. Previous studies identified several genes that contribute to the development of PCV; however, almost all reported genetic risk factors for PCV are the same as for AMD [13–15], and this suggests that AMD and PCV share, at least in part, the same genetic background.

Studies in cohorts from both the United Kingdom and the United States have shown that the complement component 1 inhibitor (*SERPING1*) gene is positively associated with AMD [16]. However,

Table 1. Characteristics of the Study Population.

		Cases		Controls	
		tAMD	PCV	Control 1*	Control 2†
No. of participants		401	510	336	1194
Age	Mean ± SD	77.38±8.39	74.98±7.77	74.16±8.42	50.34±15.9
Gender	Men	287	372	142	493
	Women	114	138	194	701

tAMD, typical age-related macular degeneration; PCV, polypoidal choroidal vasculopathy; SD, standard deviation.
*Cataract patients without age-related maculopathy.
†Healthy Japanese individuals.
doi:10.1371/journal.pone.0019108.t001

another study in a larger cohort (n = 7723 and 2327) which involved the same population could not replicate the finding of the previous study [17,18]. Recently, Lee et al. have shown that *SERPING1* is positively associated with AMD in Caucasians [19], but whether this gene is truly associated with AMD remains controversial.

Furthermore, the association of *SERPING1* with AMD has been evaluated also in Asians. Lu et al. examined the association in 194 AMD patients and 285 controls and reported that *SERPING1* is not associated with AMD in the Chinese population [20]. The association between PCV and *SERPING1* has also been evaluated in a smaller Chinese cohort (118 patients and 115 controls), also with negative findings [21]. So far, all Asian studies for *SERPING1* did use smaller cohorts than those of original studies and not consider their statistical power. For evaluating the true gene-disease association, it would be helpful to replicate the positive association reported in previous studies using a different ethnic cohort. The aim of this study, which involved a relatively large number of participants, was to investigate whether the *SERPING1* gene variants are associated with typical AMD or PCV in a Japanese population.

Materials and Methods

All procedures in this study adhered to the tenets of the Declaration of Helsinki. This study was approved by the Ethics Committee of each institute involved (Kyoto University Graduate School and Faculty of Medicine, Ethics Committee, the Ethical

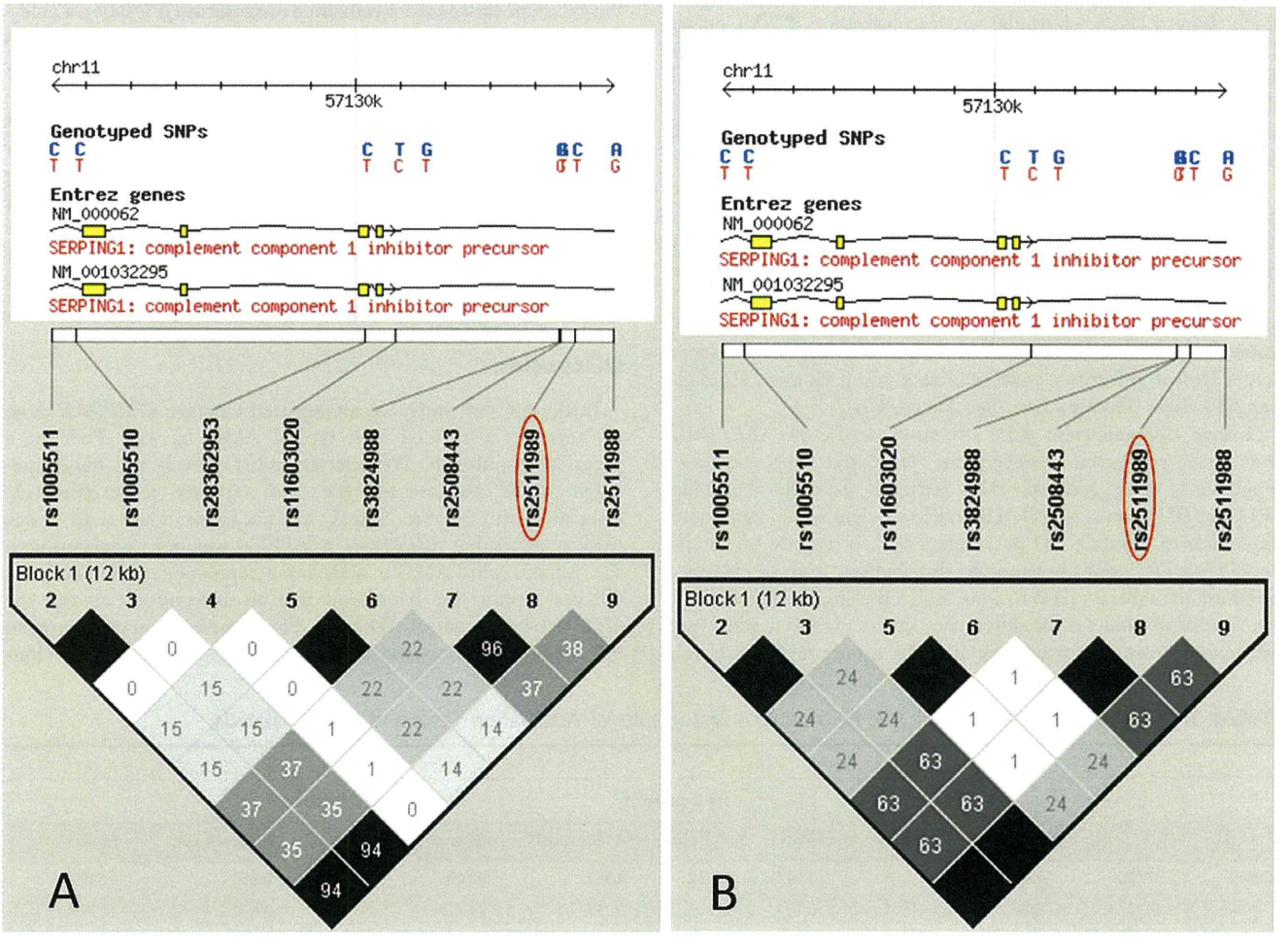

Figure 1. Linkage disequilibrium (LD) structure across the complement component 1 inhibitor (*SERPING1*) gene in Caucasian and Japanese populations. Genotype data were retrieved from HapMap CEU (Utah residents with ancestry from northern and western Europe; A) and JPT (Japanese in Tokyo, Japan; B) data sets. Haplotype blocks were determined using the "four-gamete rule" option in Haploview; all HapMap single nucleotide polymorphisms on *SERPING1* gene are in the same block in both populations. Each box provides estimated statistics of the coefficient of determination (r^2), with darker shades representing stronger LD.
doi:10.1371/journal.pone.0019108.g001

Committee of Fukushima Medical University, the Ethical Committee of Kobe City Medical Center General Hospital, the Ethical Committee of Ozaki Eye Hospital, the Ethical Committee of the Otsu Red Cross Hospital, the Ethical Committee of Nagahama City Hospital, and the Ethical Committee at Aichi Cancer Center). All of the patients were fully informed about the purpose and procedures of this study, and written consent was obtained from each.

In this study, 401 patients with typical AMD and 510 patients with PCV were recruited from the Department of Ophthalmology at Kyoto University Hospital, Fukushima Medical University Hospital, and Kobe City Medical Center General Hospital. The control group included 2 populations: (1) 336 individuals who underwent cataract surgery and had no age-related maculopathy (ARM) (Control 1) were recruited from the Department of Ophthalmology, Kyoto University Hospital, Ozaki Eye Hospital, Japanese Red Cross Otsu Hospital, and Nagahama City Hospital; and (2) 1194 healthy individuals who were recruited from the Aichi Cancer Center Research Institute as the general population control (Control 2). AMD and ARM were defined according to the International Classification System for ARM and AMD [22]. The diagnosis of PCV was based on indocyanine green angiography, which showed a branching vascular network that terminated in polypoidal swelling. Typical AMD were late AMD which showed classic choroidal neovascularization (CNV), occult CNV, or both. All diagnoses were made by 3 retina specialists (K.Y., A.T., and A.O.); a fourth specialist (N.Y.) was consulted when the subtype classification could not be decided on by the initial 3 reviewers. All of the subjects were unrelated and were of the Japanese descent.

Genomic DNAs were isolated from the peripheral blood of the subjects by using a DNA extraction kit (QuickGene-610L, Fujifilm, Minato, Tokyo, Japan). The samples of all the patients with typical AMD and PCV and of cataract patients were genotyped using a Taqman single nucleotide polymorphism (SNP) assay with the ABI PRISM 7700 system (Applied Biosystems, Foster City, CA). The individuals recruited from the Aichi Cancer Center Research Institute were genotyped using Illumina HumanHap 610 chips (Illumina Inc., San Diego, CA).

Linkage disequilibrium (LD) structures across the *SERPING1* gene were compared between the Caucasian and Japanese populations, using genotype data retrieved from the HapMap CEU and JPT data sets [23]. The retrieved data were loaded into Haploview to estimate LD parameters and to identify haplotype blocks [24]. Deviations in genotype distributions from the Hardy–Weinberg equilibrium (HWE) were assessed using the HWE exact test. Statistical analyses for differences in the observed genotypic distribution were performed by the chi square test for trend; logistic regression analysis was performed for age and gender adjustments. The statistical power calculation was performed using QUANTO version 1.2 [25]. P values less than 0.05 were considered statistically significant.

Results

The demographic details of the study population are presented in Table 1. Because all SNPs of the *SERPING1* gene are in the same haplotype block, rs2511989 was selected as the haplotype-tagging SNP; rs2511989 was reported to be associated with the risk of AMD in previous studies [16,19] (Fig. 1). Details of allele and genotype counts and summary statistics for rs2511989 are shown in Table 2. The success rate of genotyping of rs2511989 was 98.1%, and the distributions of the genotypes for all study groups were in the Hardy–Weinberg equilibrium ($P>0.05$). Although we compared the genotype distributions of rs2511989 in typical AMD and PCV patients against 2 independent control groups (cataract patients without ARM and healthy Japanese individuals), *SERPING1* rs2511989 was not significantly associated with typical AMD ($P=0.932$ and 0.513, respectively); furthermore, it was not significantly associated with PCV ($P=0.505$ and 0.141, respectively). After correction for age and gender differences based on a logistic regression model, the difference in the genotype distributions remained insignificant ($P>0.05$). Table 3 shows the odds ratios adjusted for age and gender under various genetic models. We could not find a significant association in any genetic model.

Next, we calculated our statistical power to detect an association of a risk allele with the odds ratio reported in the previous study that investigated the association of rs2511989 with developing AMD. When we targeted the original study reported by Ennis (odds ratio 0.63) [16], our sample size had more than 90% power to detect the association (Table 2). In addition, the statistical power calculation revealed that our sample size could detect the gene-disease association for an odds ratio of 0.797 by more than 80%.

Discussion

In the present study, we investigated whether *SERPING1* gene variants are associated with typical AMD or with PCV in a Japanese population. We selected rs2511989 as the haplotype-tagging SNP, because this has been reported to be positively associated with the risk of AMD in Caucasians. The results of this study showed that *SERPING1* rs2511989 was not associated with the risk for typical AMD in a Japanese population; thus, the results did not support the hypothesis that an association between the *SERPING1* gene and AMD exists. Our sample size had more than 90% power to detect the association determined in the previous

Table 2. *SERPING1* rs2511989 Genotypic Distributions and Results of Association Tests and Power Analysis.

						vs Control 1			vs Control 2		
		GG	GA	AA	MAF	P Value	Adjusted P*	Power†	P Value	Adjusted P*	Power†
Cases	tAMD	293	102	6	0.142	0.932	0.687	93.6%	0.513	0.860	99.3%
	PCV	380	125	5	0.132	0.505	0.855	95.7%	0.141	0.678	99.2%
Controls	Control 1	248	76	10	0.144	-	-	-	-	-	-
	Control 2	859	308	27	0.152	-	-	-	-	-	-

tAMD, typical age-related macular degeneration; PCV, polypoidal choroidal vasculopathy; MAF, minor allele frequency.
*Adjusted for age and gender.
†Statistical power for detecting the association reported in the previous study (odds ratio 0.63).
doi:10.1371/journal.pone.0019108.t002

Table 3. Odds Ratios in Various Genetic Models.

		Adjusted Odds Ratio (95% Confidence Interval)*	
Group	**Model**	**vs tAMD**	**vs PCV**
Control 1	Additive	0.938 (0.687–1.281)	0.972 (0.72–1.312)
	Dominant	1.283 (0.746–2.204)	0.598 (0.338–1.056)
	Recessive	0.934 (0.783–1.114)	1.283 (0.746–2.204)
Control 2	Additive	1.034 (0.716–1.491)	0.933 (0.673–1.294)
	Dominant	0.940 (0.470–1.879)	0.709 (0.349–1.440)
	Recessive	1.025 (0.839–1.254)	0.983 (0.823–1.174)

*Adjusted for age and gender.
tAMD, typical age-related macular degeneration; PCV, polypoidal choroidal vasculopathy.
doi:10.1371/journal.pone.0019108.t003

study in a Caucasian cohort (odds ratio 0.63) [16]. Furthermore, we found no evidence to support the role played by *SERPING1* rs2511989 in the susceptibility to PCV, and this finding is in agreement with that of the previous study in a Chinese population [21].

The reported association between AMD and *SERPING1* rs2511989 is shown in Table 4. The size of our Japanese cohort was similar to that of the original study [16]. Furthermore, the statistical power calculation revealed that our sample size could detect the gene-disease association for an odds ratio of 0.797 by more than 80%. Had there been a true protective effect of *SERPING1* gene variants for developing AMD at the same level as was reported in previous studies [16,19], the statistical power of our study would have detected such an association. Differences in the ethnicities of subjects might be 1 reason for the difference observed between the results of this study in a Japanese cohort and those of the previous study in a Caucasian cohort. Frequency of the minor allele of rs2511989 was reportedly greater in the earlier study in a Caucasian population than that of the present study in a Japanese population. In fact, in reference to the allele frequency data from the HapMap, all genetic variants across the *SERPING1* gene showed smaller minor allele frequency in Japanese than in Caucasians.

Another possible explanation for the differences between our findings and those of other studies in different ethnic cohorts may include a difference in the phenotypes of AMD. Numerous studies have reported that distinguishing features of Asian AMD include male predominance, unilateral presentation, comparatively low incidence of soft drusen, and greater prevalence of neovascular AMD and PCV [26–29]. To address these concerns, we classified AMD patients into those with typical AMD and those with PCV, but the possible hidden differences in the phenotypes cannot be excluded. Alternatively, considering the fact that genetic variants that are associated with a particular disease in 1 population may not necessarily be associated in another population [30–32]; moreover, it is possible that gene-disease association of *SERPING1* in populations from East Asia is very weak or absent as compared with Caucasian populations.

In this study, we used general population-based controls (Control 2). The possibility exists that some of the eyes in the control 2 group might have or develop AMD or PCV, and this might be a possible explanation for the negative results in this study. However, because the prevalence of AMD in the general population is estimated to be 0.5% in the Japanese population [33], the loss of the statistical power of association analysis must be negligible. In addition, we also performed a subset analysis on

Table 4. Comparison of Association Observed between AMD and *SERPING1* rs2511989.

Subject Group		Current Study (JP)			Mayo Subjects (US)		AREDS Subjects (US)		Ennis et al. (UK)		Ennis et al. (US)		Lee et al. (US)		Lu et al. (CH)	
Subjects		**Case**	**Control 1**	**Control 2**	**Case**	**Control**	**Case**	**Control**	**Case**	**Control**	**Case**	**Control**	**Case**	**Control**	**Case**	**Control**
No. of participants		401	336	1194	470	310	1221	295	479	479	248	252	556	256	194	285
Allele count	G	688	572	2026	569	363	1435	357	597	500	322	282	669	283	336	493
	A	114	96	362	371	257	1007	233	355	454	174	222	413	229	52	69
Genotype count	GG	293	248	859	179	103	436	115	191	132	100	79	213	74	147	215
	GA	102	76	308	211	157	563	127	215	236	122	124	273	135	42	63
	AA	6	10	27	80	50	222	53	70	109	26	49	70	47	5	3
MAF		0.142	0.144	0.152	0.395	0.415	0.412	0.395	0.373	0.475	0.351	0.441	0.382	0.447	0.134	0.123
P values		-	0.932	0.513	-	0.46	-	0.41	-	5.4×10^{-6}	-	0.0037	-	0.011	-	0.61

MAF, minor allele frequency.
doi:10.1371/journal.pone.0019108.t004

controls 2 with 55 years of age or older to minimize the possibility that some of the eyes in the control group might develop AMD or PCV. However, no new significant differences in the genotypic distributions were found in the current study (data not shown). Thus, we concluded that the result of the analysis using control 2 is valuable as reference data which supports a lack of association between *SERPING1* and both typical AMD and PCV in a Japanese population. Another limitation is about geographical difference of Control 1, which may influence genetic background of the participants. However, because the Japanese population has been reported to have a rather small genetic diversity, according to data from the SNP discovery project in Japan [34], geographical difference should not be affect our statistical results.

In conclusion, this study showed a lack of association between *SERPING1* and both typical AMD and PCV in a Japanese population; thus, the results suggest that *SERPING1* does not play a significant role in the risk of developing AMD or PCV in Japanese.

Acknowledgments

We thank the patients and the controls who participated in this study, as well as Takahisa Kawaguchi at the Center for Genomic Medicine/Inserm U.852 for his assistance in data management. We also thank the following clinicians for their help in the recruitment of patients and controls for our study: Dr. Hiroshi Tamura and Dr. Sotaro Ooto, Kyoto University Hospital; Dr. Yasuo Kurimoto, Kobe City Medical Center General Hospital; Dr. Kuniharu Saito, Fukushima Medical University; Dr. Mineo Ozaki, Ozaki Eye Hospital; Dr. Shoji Kuriyama, Otsu Red-Cross Hospital; and Dr. Yoshiki Ueda, Nagahama City Hospital.

Author Contributions

Conceived and designed the experiments: IN KY HN NY. Performed the experiments: IN NG HN HH. Analyzed the data: IN RY. Contributed reagents/materials/analysis tools: IN KY RY NG HN HH AT AO MS TI AO KM KT FM NY. Wrote the paper: IN KY RY.

References

1. Klein R, Klein BE, Jensen SC, Meuer SM (1997) The five-year incidence and progression of age-related maculopathy: the Beaver Dam Eye Study. Ophthalmology 104: 7–21.
2. Klein RJ, Zeiss C, Chew EY, Tsai JY, Sackler RS, et al. (2005) Complement factor H polymorphism in age-related macular degeneration. Science 308: 385–389.
3. Edwards AO, Ritter R, 3rd, Abel KJ, Manning A, Panhuysen C, et al. (2005) Complement factor H polymorphism and age-related macular degeneration. Science 308: 421–424.
4. Haines JL, Hauser MA, Schmidt S, Scott WK, Olson LM, et al. (2005) Complement factor H variant increases the risk of age-related macular degeneration. Science 308: 419–421.
5. Yang Z, Camp NJ, Sun H, Tong Z, Gibbs D, et al. (2006) A variant of the HTRA1 gene increases susceptibility to age-related macular degeneration. Science 314: 992–993.
6. Dewan A, Liu M, Hartman S, Zhang SS, Liu DT, et al. (2006) HTRA1 promoter polymorphism in wet age-related macular degeneration. Science 314: 989–992.
7. Seitsonen S, Lemmela S, Holopainen J, Tommila P, Ranta P, et al. (2006) Analysis of variants in the complement factor H, the elongation of very long chain fatty acids-like 4 and the hemicentin 1 genes of age-related macular degeneration in the Finnish population. Mol Vis 12: 796–801.
8. Gotoh N, Nakanishi H, Hayashi H, Yamada R, Otani A, et al. (2009) ARMS2 (LOC387715) variants in Japanese patients with exudative age-related macular degeneration and polypoidal choroidal vasculopathy. Am J Ophthalmol 147: 1037–1041.
9. Hayashi H, Yamashiro K, Gotoh N, Nakanishi H, Nakata I, et al. (2010) CFH and ARMS2 Variations in age-related macular degeneration, polypoidal choroidal vasculopathy, and retinal angiomatous proliferation. Invest Ophthalmol Vis Sci 51: 5914–5919.
10. Simonelli F, Frisso G, Testa F, di Fiore R, Vitale DF, et al. (2006) Polymorphism p.402Y>H in the complement factor H protein is a risk factor for age related macular degeneration in an Italian population. Br J Ophthalmol 90: 1142–1145.
11. Sho K, Takahashi K, Yamada H, Wada M, Nagai Y, et al. (2003) Polypoidal choroidal vasculopathy: incidence, demographic features, and clinical characteristics. Arch Ophthalmol 121: 1392–1396.
12. Terasaki H, Miyake Y, Suzuki T, Nakamura M, Nagasaka T (2002) Polypoidal choroidal vasculopathy treated with macular translocation: clinical pathological correlation. Br J Ophthalmol 86: 321–327.
13. Kondo N, Honda S, Kuno S, Negi A (2009) Coding variant I62V in the complement factor H gene is strongly associated with polypoidal choroidal vasculopathy. Ophthalmology 116: 304–310.
14. Gotoh N, Yamada R, Nakanishi H, Saito M, Iida T, et al. (2008) Correlation between CFH Y402H and HTRA1 rs11200638 genotype to typical exudative age-related macular degeneration and polypoidal choroidal vasculopathy phenotype in the Japanese population. Clin Experiment Ophthalmol 36: 437–442.
15. Lee KY, Vithana EN, Mathur R, Yong VH, Yeo IY, et al. (2008) Association analysis of CFH, C2, BF, and HTRA1 gene polymorphisms in Chinese patients with polypoidal choroidal vasculopathy. Invest Ophthalmol Vis Sci 49: 2613–2619.
16. Ennis S, Jomary C, Mullins R, Cree A, Chen X, et al. (2008) Association between the SERPING1 gene and age-related macular degeneration: a two-stage case-control study. Lancet 372: 1828–1834.
17. Allikmets R, Dean M, Hageman GS, Baird PN, Klaver CC, et al. (2009) The SERPING1 gene and age-related macular degeneration. Lancet 374: 875–876.
18. Park KH, Ryu E, Tosakulwong N, Wu Y, Edwards AO (2009) Common variation in the SERPING1 gene is not associated with age-related macular degeneration in two independent groups of subjects. Mol Vis 15: 200–207.
19. Lee AY, Kulkarni M, Fang AM, Edelstein S, Osborn MP, et al. (2010) The effect of genetic variants in SERPING1 on the risk of neovascular age-related macular degeneration. Br J Ophthalmol 94: 915–917.
20. Lu F, Zhao P, Fan Y, Tang S, Hu J, et al. (2010) An association study of SERPING1 gene and age-related macular degeneration in a Han Chinese population. Mol Vis 16: 1–6.
21. Li M, Wen F, Zuo C, Zhang X, Chen H, et al. (2010) SERPING1 polymorphisms in polypoidal choroidal vasculopathy. Mol Vis 16: 231–239.
22. Bird AC, Bressler NM, Bressler SB, Chisholm IH, Coscas G, et al. (1995) An international classification and grading system for age-related maculopathy and age-related macular degeneration. The International ARM Epidemiological Study Group. Surv Ophthalmol 39: 367–374.
23. International HapMap Consortium (2003) The International HapMap Project. Nature 426: 789–796.
24. Barrett JC, Fry B, Maller J, Daly MJ (2005) Haploview: analysis and visualization of LD and haplotype maps. Bioinformatics 21: 263–265.
25. Gauderman WJ (2002) Sample size requirements for matched case-control studies of gene-environment interaction. Statistics in Medicine 21: 35–50.
26. Chang TS, Hay D, Courtright P (1999) Age-related macular degeneration in Chinese-Canadians. Can J Ophthalmol 34: 266–271.
27. Bird AC (2003) The Bowman lecture. Towards an understanding of age-related macular disease. Eye (Lond) 17: 457–466.
28. Mori K, Horie-Inoue K, Gehlbach PL, Takita H, Kabasawa S, et al. (2010) Phenotype and genotype characteristics of age-related macular degeneration in a Japanese population. Ophthalmology 117: 928–938.
29. Maruko I, Iida T, Saito M, Nagayama D, Saito K (2007) Clinical characteristics of exudative age-related macular degeneration in Japanese patients. Am J Ophthalmol 144: 15–22.
30. Helgason A, Pálsson S, Thorleifsson G, Grant SF, Emilsson V, et al. (2007) Refining the impact of TCF7L2 gene variants on type 2 diabetes and adaptive evolution. Nat Genet 39: 218–225.
31. Chandak GR, Janipalli CS, Bhaskar S, Kulkarni SR, Mohankrishna P, et al. (2007) Common variants in the TCF7L2 gene are strongly associated with type 2 diabetes mellitus in the Indian population. Diabetologia 50: 63–67.
32. Horikoshi M, Hara K, Ito C, Nagai R, Froguel P, et al. (2007) A genetic variation of the transcription factor 7-like 2 gene is associated with risk of type 2 diabetes in the Japanese population. Diabetologia 50: 747–751.
33. Kawasaki R, Wang JJ, Ji GJ, Taylor B, Oizumi T, et al. (2008) Prevalence and risk factors for age-related macular degeneration in an adult Japanese population: the Funagata study. Ophthalmology 115: –1381, 1381 e1371-1372.
34. Haga H, Yamada R, Ohnishi Y, Nakamura Y, Tanaka T (2002) Gene-based SNP discovery as part of the Japanese Millennium Genome Project: identification of 190,562 genetic variations in the human genome. Single-nucleotide polymorphism. J Hum Genet 47: 605–610.

Myelin Basic Protein as a Novel Genetic Risk Factor in Rheumatoid Arthritis—A Genome-Wide Study Combined with Immunological Analyses

Chikashi Terao[1,2,3], Koichiro Ohmura[2], Masaki Katayama[2], Meiko Takahashi[1], Miki Kokubo[1,4], Gora Diop[1], Yoshinobu Toda[5], Natsuki Yamamoto[2], Human Disease Genomics Working Group[¶a], Rheumatoid Arthritis (RA) Clinical and Genetic Study Consortium[¶b], Reiko Shinkura[6], Masakazu Shimizu[2], Ivo Gut[7], Simon Heath[7], Inga Melchers[8], Toshiaki Manabe[9], Mark Lathrop[7,10], Tsuneyo Mimori[2], Ryo Yamada[1,11], Fumihiko Matsuda[1,4,12]*

1 Center for Genomic Medicine, Graduate School of Medicine, Kyoto University, Kyoto, Japan, **2** Department of Rheumatology and Clinical Immunology, Graduate School of Medicine, Kyoto University, Kyoto, Japan, **3** Global Centers of Excellence (COE) program, Kyoto University Graduate School of Medicine, Kyoto, Japan, **4** Core Research of Evolutional Science and Technology (CREST) program, Japan Science and Technology Agency, Kawaguchi, Saitama, Japan, **5** Center for Anatomical Studies, Graduate School of Medicine, Kyoto University, Kyoto, Japan, **6** Department of Immunology and Genomic Medicine, Kyoto University Graduate School of Medicine, Kyoto, Japan, **7** Commisariat a l'energie Atomique (CEA), Institut Genomique, Centre National de Genotypage, Evry, France, **8** Clinical Research Unit for Rheumatology, University Medical Center, Freiburg, Germany, **9** Laboratory of Diagnostic Pathology, Graduate School of Medicine, Kyoto University, Kyoto, Japan, **10** Fondation Jean Dausset, Centre d'Etude du Polymorphisme Humain, Paris, France, **11** Unit of Statistical Genetics, Center for Genomic Medicine Graduate School of Medicine Kyoto University, Kyoto, Japan, **12** Institut National de la Sante et de la Recherche Medicale (INSERM) Unite U852, Kyoto University Graduate School of Medicine, Kyoto, Japan

Abstract

Rheumatoid arthritis (RA) is a major cause of adult chronic inflammatory arthritis and a typical complex trait. Although several genetic determinants have been identified, they account for only a part of the genetic susceptibility. We conducted a genome-wide association study of RA in Japanese using 225,079 SNPs genotyped in 990 cases and 1,236 controls from two independent collections (658 cases and 934 controls in collection1; 332 cases and 302 controls in collection2), followed by replication studies in two additional collections (874 cases and 855 controls in collection3; 1,264 cases and 948 controls in collection4). SNPs showing $p<0.005$ in the first two collections and $p<10^{-4}$ by meta-analysis were further genotyped in the latter two collections. A novel risk variant, rs2000811, in intron2 of the myelin basic protein (*MBP*) at chromosome 18q23 showed strong association with RA ($p=2.7\times10^{-8}$, OR 1.23, 95% CI: 1.14–1.32). The transcription of *MBP* was significantly elevated with the risk allele compared to the alternative allele ($p<0.001$). We also established by immunohistochemistry that MBP was expressed in the synovial lining layer of RA patients, the main target of inflammation in the disease. Circulating autoantibody against MBP derived from human brain was quantified by ELISA between patients with RA, other connective tissue diseases and healthy controls. As a result, the titer of anti-MBP antibody was markedly higher in plasma of RA patients compared to healthy controls ($p<0.001$) and patients with other connective tissue disorders ($p<0.001$). ELISA experiment using citrullinated recombinant MBP revealed that a large fraction of anti-MBP antibody in RA patients recognized citrullinated MBP. This is the first report of a genetic study in RA implicating MBP as a potential autoantigen and its involvement in pathogenesis of the disease.

Citation: Terao C, Ohmura K, Katayama M, Takahashi M, Kokubo M, et al. (2011) Myelin Basic Protein as a Novel Genetic Risk Factor in Rheumatoid Arthritis—A Genome-Wide Study Combined with Immunological Analyses. PLoS ONE 6(6): e20457. doi:10.1371/journal.pone.0020457

Editor: Amanda Ewart Toland, Ohio State University Medical Center, United States of America

Received March 10, 2011; **Accepted** April 21, 2011; **Published** June 3, 2011

Funding: C.T. is an associate fellow of Global Centers of Excellence program supported by the Ministry of Education, Culture, Sports, Science, and Technology (MEXT), Japan (http://www.mext.go.jp/english/). G.D. is a postdoctoral fellow of Japan Society for the Promotion of Science (JSPS, http://www.jsps.go.jp/english/) and M.A. is a research member of Core University Program supported by JSPS (http://www.jsps.go.jp/english/). The study was supported in part by Core Research of Evolutional Science & Technology (http://www.jst.go.jp/kisoken/crest/en/index.html), Solution-Oriented Research for Science and Technology (http://www.jst.go.jp/kisoken/sorst/en/index.html), Japan Science and Technology Agency (http://www.jst.go.jp/EN/index.html), and by grants-in-aid for scientific research from MEXT (http://www.mext.go.jp/english/) and from the Ministry of Health, Labour and Welfare in Japan (http://www.mhlw.go.jp/english/index.html), by the Institut National de la Sante et de la Recherche Medicale in France (http://english.inserm.fr/), and by Okawa Foundation for Information and Telecommunications (http://www.okawa-foundation.or.jp/e/). The funders had no role in study design, data collection and analysis, decision to publish, or preparation of the manuscript. No additional external funding received for this study.

Competing Interests: The authors have declared that no competing interests exist.

* E-mail: fumi@genome.med.kyoto-u.ac.jp

¶a Membership of the Human Disease Genomics Working Group is provided in the Acknowledgments.
¶b Membership of the RA Clinical and Genetic Study Consortium is provided in the Acknowledgments.

Introduction

Rheumatoid arthritis (RA) is the most common cause of adult inflammatory arthritis, affecting 0.5–1% of the adult population worldwide, and is associated with joint pain, dysfunction and deformity. Both genetic and environmental risk factors have been implicated in RA [1–2]. *HLA-DRB1* is a major genetic component of RA across ethnicities and is estimated to contribute to 30 to 50% of the total genetic risk [3]. However, the other risk loci identified to date show ethnic-specific patterns of disease association. Large-scale genetic analyses including genome-wide association (GWA) studies have shown that more than 20 genes such as *PTPN22*, *TRAF1/C5*, *CD40*, and *TNFAIP3* are associated with RA in populations of European descent [4–12]. A different set of non-*HLA* genes, namely, *PADI4*, *SLC22A4*, *FCRL3*, *CD244* and *CCR6* were first reported for their association with RA using Japanese DNA collections [13–17]. Among them, several genes including *CCR6*, *STAT4* and *TNFAIP3* were later proven their association beyond ethnicity [12,18–19]. On the other hand, some other genes showed strong specificity to a certain ethnic group. The association of the *PTPN22* has been repeatedly reproduced by subsequent genetic studies in Europeans [5,20–21]. However, no evidence of strong disease risk in *PTPN22* was shown in Japanese in part due to a much lower frequency of the risk allele [22]. Similarly the association of *PADI4* with RA, which has been confirmed by multiple genetic studies in Japanese and Koreans [23–24], is found to be much weaker in Europeans [25–26]. Moreover, the size of DNA collections used for GWA studies is much larger in European populations than in Japanese, suggesting the existence of unknown genetic factors in Japanese [12,17]. For these reasons, we decided to conduct a new large-scale GWA study of RA in Japanese. Independent collections of RA patients and controls were enrolled from four clinical centers in our study. The collections from two centers, totaling 990 cases and 1,241 controls, were characterized with genome-wide SNP arrays, and the data were analyzed to identify potential disease-associated loci. For replication, SNPs at these loci were examined in the two remaining collections, totaling 2,138 cases and 1,803 controls.

Results

Genome scan and validation studies

We accumulated data on 3,128 cases and 3,039 controls of four independent RA collections (termed as collections 1,2,3 and 4, Table S1). Collections 1 and 2 (totaling 990 cases and 1,236 controls) were used for GWA analysis and collections 3 and 4 (totaling 2,138 cases and 1,803 controls) were used as replication samples. Quality control of the GWA genotyping results was undertaken separately in cohorts 1 and 2 because of differences in the SNP arrays used (see Methods, Table S2). For 225,079 markers that were common between the arrays and fulfilled our inclusion criteria, we found no evidence of population stratification between cases and controls (genomic control inflation factor $\lambda = 1.03$, Figure S1). We undertook analysis of each collection individually, and a meta-analyses to pool the results in the two collections in the association analysis (see Methods for further details). We report p-values from the meta-analysis unless otherwise stated.

We found a strong association of disease risk with markers in the *HLA* complex [27] ($p = 5.0\times10^{-31}$, Table S3). Although no other chromosomal loci showed genome-wide significance, we detected evidence of association signal in *PADI4* ($p = 2.3\times10^{-5}$), as previously reported in Japanese [13,23,27] (Table S3). The association results of five reported genes in Japanese were shown in Table S4. These results support the quality of our study populations for genetic analysis. In addition, we identified 10 SNPs in five additional chromosomal regions that met our statistical criteria for testing in the replication collections ($p<0.005$ in both collections 1 and 2, and $p<10^{-4}$ in the meta-analysis). None of them showed potential association with p-value being smaller than 10^{-5} in the other Japanese GWA study [17]. From each of these regions, the SNP with the smallest p-value was selected for examination in collections 3 and 4. One of these SNPs, rs2000811 ($p = 0.0036$ in collection1; $p = 5.7\times10^{-4}$ in collection2; $p = 1.2\times10^{-5}$ in the meta-analysis) located on chromosome 18q23, was significantly associated with RA in both replication collections ($p = 0.023$ in collection3; $p = 0.0041$ in collection4, and

Table 1. Association of *MBP* locus with rheumatoid arthritis in the Japanese population.

Chr	dbSNPID	Gene	Allele	DNA Collection		Genotype counts			Success rate	HWEp	RAF**	p-value	OR	mhp***
			Ref.(A1)/Var.(A2)			A1A1	A1A2	A2A2					(95%CI)	
18q23	rs2000811	*MBP*	C/T*	1	case	203	303	136	99.8	0.25	0.45	0.0036	1.25	
					control	344	442	148	100	0.76	0.4		(1.08–1.44)	
				2	case	95	152	79	99.7	0.24	0.48	5.7×10^{-4}	1.49	
					control	120	131	46	100	0.31	0.38		(1.19–1.87)	
				3	case	283	392	182	98.1	0.034	0.44	0.023	1.17	
					control	298	404	134	97.8	0.88	0.4		(1.02–1.34)	
				4	case	393	622	233	98.7	0.63	0.44	0.0041	1.19	
					control	341	451	141	98.4	0.68	0.39		(1.06–1.35)	
				3+4	case	676	1014	415	98.5	0.32	0.44	3.0×10^{-4}	1.18	
					control	639	855	275	98.1	0.69	0.4		(1.08–1.30)	
				pooled	case	974	1469	630	98.9	0.078	0.44	4.0×10^{-8}	1.23	2.7×10^{-8}
					control	1103	1428	469	98.9	0.85	0.39		(1.14–1.32)	

*risk allele for the disease,
**risk allele frequency, and
***p-value in meta-analysis using Cochran-Mantel-Haenszel test.
doi:10.1371/journal.pone.0020457.t001

$p = 3.0 \times 10^{-4}$ in collections 3 and 4). When the four collections were combined, the evidence of association at rs2000811 exceeded genome-wide significance when evaluated either by meta-analysis ($p = 2.7 \times 10^{-8}$; OR = 1.23; 95%CI 1.14–1.32) or by pooling of the genotype counts ($p = 4.0 \times 10^{-8}$; OR = 1.23; 95%CI 1.14–1.32; see Table 1). There was no difference in the effect size among the four collections ($p = 0.28$). To be more conservative, however, we have calculated corrected *p*-values with Principle Component Analysis (PCA), using subsets of case and control collections for which individual genotypes were available (970 cases and 297 controls, for details, see Materials and Methods). There was no difference in *p*-values with and without the correction ($p = 6.5 \times 10^{-4}$ and corrected $p = 6.5 \times 10^{-4}$). The four SNPs from the other regions that were tested showed no evidence of association in collection3 for replication study (Table S5).

The disease associated marker rs2000811 is located in the second intron of the *MBP* (myelin basic protein) gene at chromosome 18q23 within a 156-kb region that contains the *MBP* gene (NCBI MapViewer, build 36.3). Linkage disequilibrium (LD) was evaluated using genotyping results obtained in collections 1 and 2; rs2000811 did not show significant LD with other markers from the region ($r^2 < 0.14$; Figure 1), or elsewhere in the genome. An imputation analysis using the Japanese HapMap data identified a SNP, rs9958028, which was 358-bp apart and in strong LD with rs2000811 ($r^2 = 0.96$), as the second strongest association. However, no other marker was in strong LD with these two markers ($r^2 = 0.35$ or smaller) (Figure S2). To determine if unidentified polymorphisms within *MBP* were in LD with rs2000811, we performed a sequencing of the exons and the promoter region of the *MBP* gene in 84 Japanese population control DNAs (Method S1). We identified 66 SNPs, 37 of which were not registered in dbSNP, and three of which were deleterious polymorphisms (Tables S6 and S7). Again, none of these polymorphisms was in strong LD with rs2000811 ($r^2 = 0.35$ or smaller) (Figure S3). An imputation analysis using the genotyping results obtained by sequencing did not discover any other polymorphisms showing stronger association signals ($p > 0.0070$) than that of rs2000811. Taken together, these data suggest that rs2000811 and/or one or more other as yet unidentified non-coding polymorphisms within or near *MBP* are responsible for the genetic association.

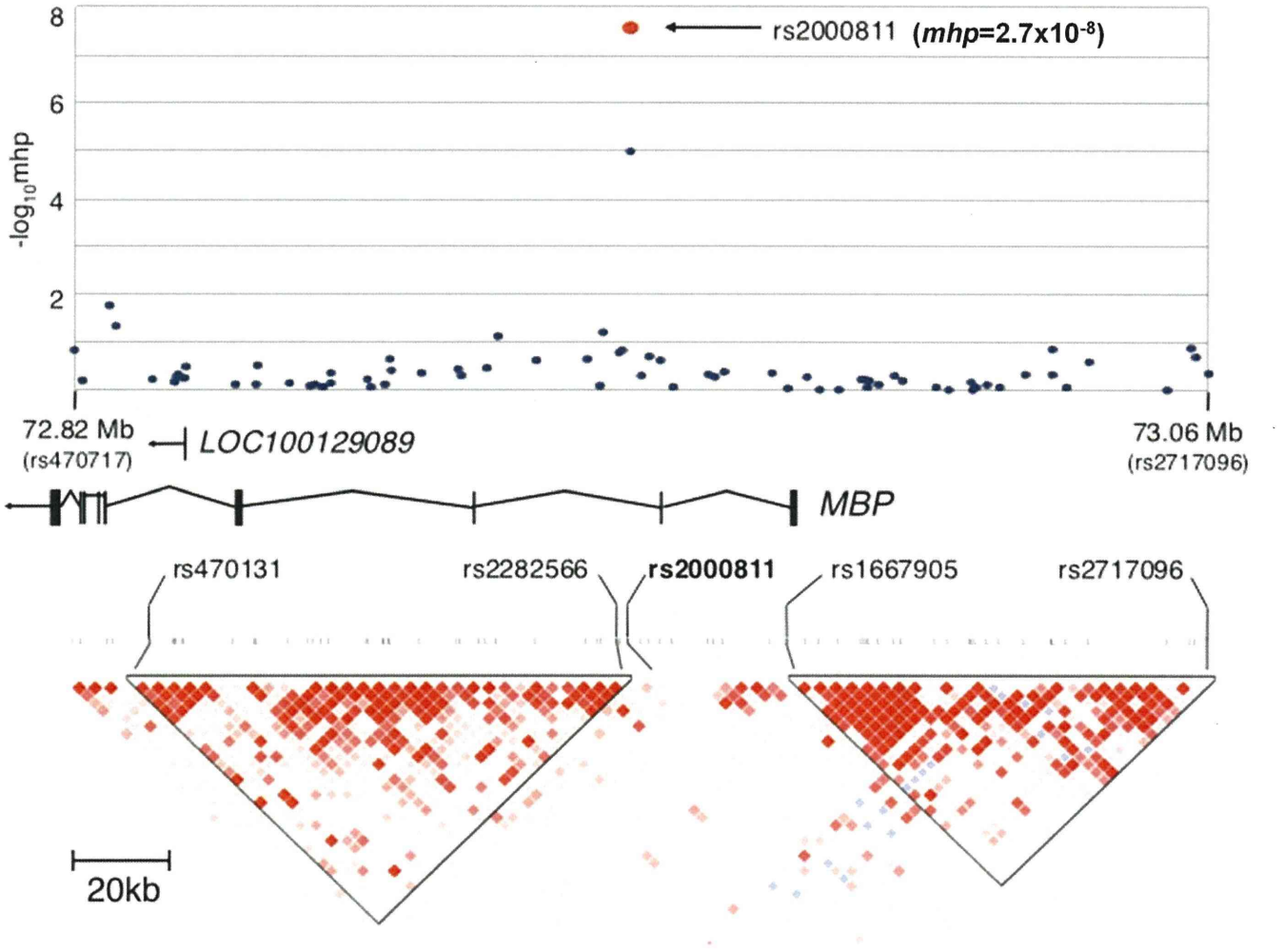

Figure 1. A schematic view of the association results and LD structure of the human *MBP* gene locus at chromosome 18q23. SNPs located between rs470131 and rs2717096 are plotted in $-\log_{10}$ scale according to their chromosomal positions and *p*-values calculated with Cochran-Mantel-Haenszel test. Red circle indicates *mhp*-value of rs2000811 by meta-analysis using the combined results of collections 1 to 4. Relative locations of the genes in the region are shown with their transcriptional orientations by arrows. LD blocks were generated using the genome scan results.

doi:10.1371/journal.pone.0020457.g001

Evaluation of MBP transcription

Quantitative RT-PCR experiments showed only very low levels of *MBP* expression in RNA from Epstein-Barr virus (EBV)-transformed human B-lymphoblastoid cell lines, and we could detect no discernable correlation of *MBP* transcript levels with different risk genotypes ($p = 0.36$, Figure S4). By a similar reason, *in-silico* expression analysis using GEO database did not return clear association [28]. However, when we performed allele-specific quantitative RT-PCR [16] using genomic DNA and cDNA of these cell lines, we observed elevated allele-specific transcription associated with the risk allele ($p<0.001$, Figure 2, for detailed procedure, see Materials and Methods). This suggests that rs2000811, and/or other variants in linkage disequilibrium with this marker, impact the quantitative pattern of *MBP* transcription. However, bioinformatics analysis identified no known *cis*-acting elements covering rs2000811 that could be inferred to have functional effects (Method S2). In addition, the alignment of the 4-kb region ranging between 2-kb centromeric and 2-kb telomeric to rs2000811 revealed that this segment has very low interspecies conservation among placental mammals.

Expression of the MBP protein in synovial tissues

Next we investigated the expression of the MBP protein in synovial tissue, as this is the main target of inflammation in RA. Microscopic observation revealed that MBP was highly expressed along the lining layer of synovial tissues in 20 out of 23 RA patients tested, while the expression of MBP was observed in only one out of five controls ($p = 0.0017$), and then generally at a weaker level (Figure 3A, B). In synovial tissue from RA patients, the detected MBP expression was weaker in synovial lining layer adjacent to the follicules of infiltrated lymphocytes (Figure 3C). In synoviocytes, the expression of MBP was mainly observed in the plasma membrane (Figure 3D).

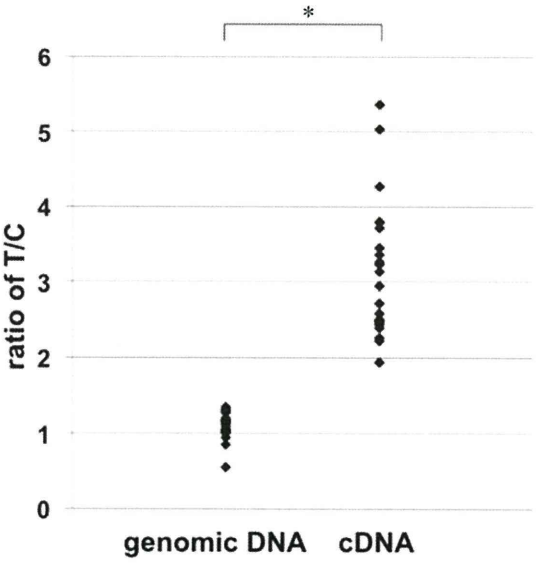

Figure 2. Allelic difference in *MBP* transcription using allele specific quantitative RT-PCR. The amount of *MBP* primary transcripts transcribed from chromosomes carrying rs2000811 risk (T) and alternative (C) alleles was compared in each cell line, and the ratio (T/C) was plotted. Genomic DNA was used as a control for equimoler biallelic representation. Experiments were done twice independently.
doi:10.1371/journal.pone.0020457.g002

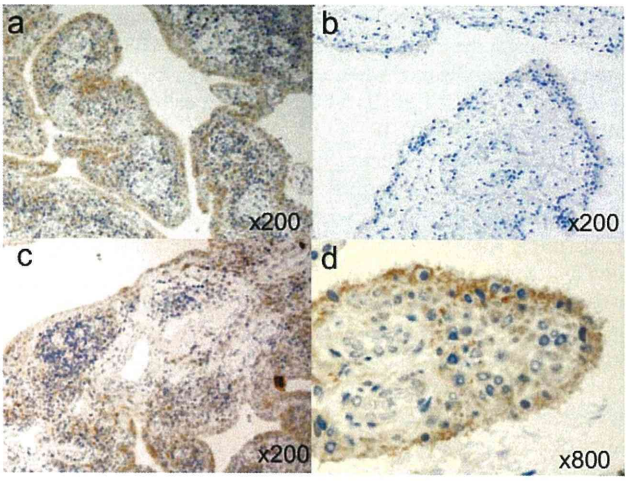

Figure 3. Immunohistochemistry of the MBP protein in human synovial tissues stained by monoclonal anti-MBP antibody. Synovial tissue of RA patients, in particular, along the synovial lining layer strongly expressed MBP (A), whereas that of non-inflammatory osteoarthritis patients was much weaker (B). The expression of MBP in the synovial lining layer was weaker near follicules of infiltrated lymphocytes (C). Localized expression of MBP was observed at the plasma membrane of synoviocytes (D).
doi:10.1371/journal.pone.0020457.g003

Quantification of antibodies to MBP in RA patients

Antibodies to MBP are the major component of autoantibodies in multiple sclerosis, a human autoimmunity with a neurodegenerative phenotype [29]. To assess a possible association of circulating antibodies to MBP with RA, we quantified these in plasma from 323 RA cases, 131 healthy controls and 162 patients with other connective tissue diseases (disease controls) by Enzyme-linked immunosorbent assay (ELISA) with MBP purified from human brain as antigen. The average levels of anti-MBP antibody in plasma of RA patients were much higher than those of healthy controls and patients with seven other connective tissue diseases ($p<0.001$; Figure 4A). Specificity in detection of anti-MBP antibody in ELISA experiments was confirmed by immunoblotting using plasma of a subset of RA patients and controls (Figure S5, Method S3). We also confirmed that the enhancement of ELISA signals by non-specific binding of IgG- and IgM-RF in patients' sera was negligible (for details, see Method S4 and Figure S6).

Amino acid analysis of the MBP protein derived from human brain showed that approximately 21% (citrulline/arginine = 6.0/23.1) of the arginine residues in MBP was citrullinated in human brain under physiological conditions (Method S5). It is possible that anti-MBP antibody recognizes and binds to citrullinated MBP protein. We then performed ELISA using recombinant MBP protein and compared the antibody titers with those of human brain-derived MBP. We could not observe correlation between the two results ($r = -0.19$, Figure 4B). However, when we used recombinant MBP protein artificially citrullinated *in-vitro*, the ELISA results showed strong correlation in titers of the autoantibody ($r = 0.88$, Figure 4C). From these results, we concluded that higher levels of anti-MBP antibody in RA patients than in healthy controls and in patients with other connective tissue diseases was attributed to autoantibodies binding to citrullinated MBP.

Discussion

We conducted a large-scale GWA-based genetic study of RA in the Japanese population. A genome scan of 225,079 SNPs in two